

The Late Middle Pleistocene mammalian fauna of Oumm Qatafa Cave, Judean Desert: taxonomy, taphonomy and palaeoenvironment

NIMROD MAROM,^{1*} IGNACIO A. LAZAGABASTER,^{1,2} ROEE SHAFIR,¹ FILIPE NATALIO,³ VERA EISENMANN⁴ and LIORA KOLSKA HORWITZ⁵

¹School of Archaeology and Maritime Cultures & the Recanati Institute for Maritime Studies, University of Haifa, Haifa, Israel

²Museum für Naturkunde, Leibniz Institute for Research on Evolution and Biodiversity at the Humboldt University Berlin, Berlin, Germany

³Weizmann Institute of Science, Rehovot, Israel

⁴Unité Mixte de Recherche 5143 du Centre National de la Recherche Scientifique, CP 38, Département Histoire de la Terre, Paris, France

⁵National Natural History Collections, The Hebrew University of Jerusalem, Jerusalem, Israel

Received 6 October 2021; Revised 13 January 2022; Accepted 26 January 2022

ABSTRACT: The Middle Pleistocene archaeological record of the southern Levant has proven key to understanding human evolution and intercontinental faunal biogeography. Knowledge of archaeological sites of that period in the southern Levant is biased, with most Middle Pleistocene localities in the Mediterranean areas in the north, despite the mosaic of environments that mark the entire region. A key Middle Pleistocene location in the Judean Desert – on the eastern margin of the Mediterranean zone – is the site of Oumm Qatafa, excavated in the early 1900s, which yielded a faunal collection spanning an estimated time period of 600–200 kya. Here, we present a revised taxonomy of the macromammalian fauna from the site, discuss the palaeoenvironmental implications of this assemblage, and relate the finds to other Pleistocene sites from the Levant. These data enable a more precise palaeoenvironmental reconstruction which attests to an open landscape, but with the addition of a mesic Mediterranean component close by. In addition, detailed taphonomic observations on butchery marks and Fourier transform infrared spectroscopy analysis of burnt bone link the fauna for the first time to anthropogenic activities in the cave.

© 2022 The Authors *Journal of Quaternary Science* Published by John Wiley & Sons Ltd

KEYWORDS: archaeology; early fire; fauna; Levant; palaeontology; Quaternary

Introduction

The southern Levant, encompassing the modern-day boundaries of Lebanon, southern Syria, Jordan, Israel, and the Palestinian Authority, is characterised by the highly heterogeneous nature of its topography, climate, environment and fauna (Fig. 1). During the Pleistocene, the region experienced climatic fluctuations that have affected the boundaries of its different phytogeographic zones, which include Mediterranean, Irano-Turanian, Sahara-Arabian and Sudanian enclaves (Danin 1988; Horowitz 1988, 1989). The rich habitat diversity and the geographical position of the Levant as a dispersal route between Eurasia and Africa is reflected in its present and past faunal composition (Bar-Oz and Weissbrod 2017; Bar-Yosef and Belmaker 2011; Bate 1937; Lazagabaster *et al.* 2021a, b, 2022; Orbach and Yeshurun 2019; Stiner *et al.* 2009; Tchernov 1988, 1998). Thus, Pleistocene sites contain typical large Eurasian mammals (e.g. aurochs, equid, cervid, wild boar, brown bear) alongside characteristic African species (elephant, hippopotamus, gazelle, hartebeest, Cape hunting dog, crested rat). The salient location as a biogeographical corridor has also made the Levant and its Pleistocene archaeological sites a crucial window into the movement, evolution and arrangement of past human populations (e.g. Bar-Yosef and Belfer-Cohen 2001; Goren-Inbar and Speth 2004; Hershkovitz *et al.*, 2015, 2018). Middle–Late

Pleistocene archaeological sites in the southern Levant, however, are concentrated in the Mediterranean areas of the north and northwest, while those in the arid regions located to the east and south (such as the Judean Desert) are scarce and often lack fauna. Consequently, a thorough biogeographical understanding of the southern Levant, with its sharp environmental gradients, is missing for this period.

The key Pleistocene site in the Judean Desert is the cave of Oumm Qatafa, which was excavated in the early 1900s and yielded an important archaeological sequence of the Lower Palaeolithic (Acheulian), spanning the period ~600 to 200 kya, i.e. marine isotope stages (MIS) 15–7 (Neuville 1931, 1934, 1951). The cave is currently located on the boundary zone between the hyperarid (Saharo-Arabian) Judean Desert and the Irano-Turanian steppe, grading to the xeric Mediterranean climate of the eastern slope of the Judean Mountains. This location, at the desert's edge abutting the Rift Valley, is unique among Levantine Acheulian sites. Indeed, sites are typically located along the coast, like Holon, Evron Quarry and Abri Zumoffen; in the northern valleys, such as Gesher Benot Ya'aqov and Latamne; or in the arid margins, as at Nadaouiye Aïn Askar, Bitzat Ruhama and Nahal Hesi (Fig. 1; Bar-Yosef 1994; see papers on these sites in Enzel and Bar-Yosef 2017). Thus, the macromammal assemblage from Oumm Qatafa fills a gap in the Middle Pleistocene for what is today a climatically marginal, and less researched, part of the Levant.

The palaeontological reports on the large mammalian fauna from Oumm Qatafa were published by Raymond

*Correspondence: N. Marom, as above.
Email: nmarom2@univ.haifa.ac.il

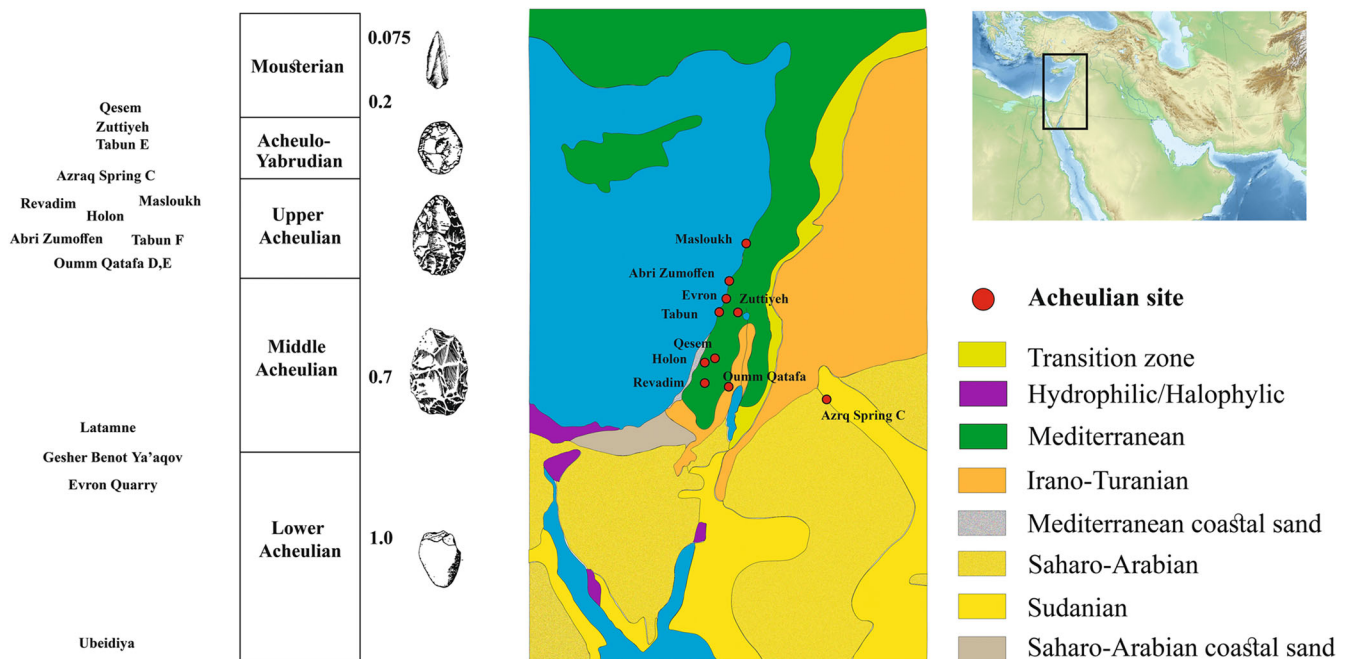


Figure 1. Regional map with modern phytogeographical zones and key Acheulian sites in relation to the chronology. Map of the Middle East modified from https://commons.wikimedia.org/wiki/File:Middle_East_topographic_map.png under Creative Commons Attribution-Share Alike 4.0 International licence; phytogeographical map drawn by NM based on Zohary (1973). [Color figure can be viewed at wileyonlinelibrary.com]

Vaufrey (1931, 1951), who provided a detailed account of the taxonomic composition of the assemblage. The 90 years that have passed since the original descriptions have seen methodological advancements in palaeozoology, combined with a richer understanding of the Middle Pleistocene context of the region, both of which called for a revision of the faunal remains from this cave. Our primary goals in this study are to refine the taxonomy as originally determined by Vaufrey, and to discuss the palaeoenvironmental implications at this key Middle Pleistocene location in view of the revision. We also strive to add systematic palaeozoological observations on taphonomy, age-at-death, and biometry that were noted in passing at that time. In so doing, we hope to provide an updated analysis which is more comparable to recently published assemblages from elsewhere in the Levant. This will expand the corpus of Acheulian faunal assemblages that can be referenced for the region and provide important comparative data.

There are, however, limitations to this study. The faunal collection from Oumm Qatafa is partial, lacking bones that were probably deemed non-diagnostic, reflecting the archaeological faunal retention practices typical of the early 1900s. Moreover, there has been a loss of information on the stratigraphic context of specimens, as well as a loss of curated material in the decades following the excavation. This situation constrains the extent of possible research questions that can be addressed using the materials at hand. For example, questions relating to the relative proportions of the representation of skeletal elements and even taxa would be difficult to address given the severe collection bias. This leaves us with three important data sets we feel are robust enough to use: firstly, a revised taxonomic list (Lyman 1986, 2015); secondly, species-specific observations on biometry, morphology and age-at-death; and, lastly, the presence or absence of bone-surface modifications to facilitate assessment of the involvement of different taphonomic agents in assemblage formation. These data sets will be employed to answer the following questions: (1) Are there species in the fauna from Middle Pleistocene Oumm Qatafa that reflect climatic conditions that are essentially different from today? (2) Do the biometric data

suggest changes in body size that could be related to climatic shifts and ecophysiological rules? and (3) Can we find taphonomic signatures suggestive of the presence, and even relative importance, of different bone accumulators in the assemblage?

The site

The karstic cave of Oumm Qatafa (also written as Umm Qatafa) is situated on the western side of Wadi Khareitoun in the Judean hills, ~40 km southeast of Jerusalem. Three deep soundings within the cave (Pits I–III) were excavated by Rene Neuville in three seasons – 1928, 1932 and 1949 (Neuville 1931, 1934, 1951). He described a depositional sequence ~12 m in depth comprising 13 stratigraphic layers, with a heavy rockfall throughout Layer E2 which separates Layers G to E3 on the one hand, from Layers D2 to A on the other (Fig. 2):

Layers H to J: Archaeologically sterile deposits.

Layers G2 and G1: Partially decomposed limestone. According to Neuville (1951), artefacts in this layer were scarce but belonged to Neuville's 'Tayacian I', an early Acheulian industry. Rodents were the only faunal remains.

Layers F to E3: This is a dark brown clay with calcareous concretions. According to the 1951 publication, the thickness of Layer F ranged from 1 to 2.75 m while Layer E3 was ~40 cm thick.

Layers F to E3 represent Neuville's 'Tayacian II' (early Acheulian industry), comprising artefacts manufactured using improved knapping techniques compared with Layer G. Based on parallels for Oumm Qatafa with the Tayacian industry at the sites of Hummal Layer 13 and Tabun Cave Layer G, we estimate the age of these lower layers in the cave to be ~600 Ka (Mercier *et al.* 2000; Wojtczak and Le Tensorer 2018).

Layers E2–E1: The sediment in these layers was described as comprising very compact yellow-green silt with white phosphate concretions forming breccia along the cave walls. Layer E2 is marked by a substantial rockfall which was then sealed by a stalagmitic layer. Layers E2–E1 were ~1 m and 60 cm

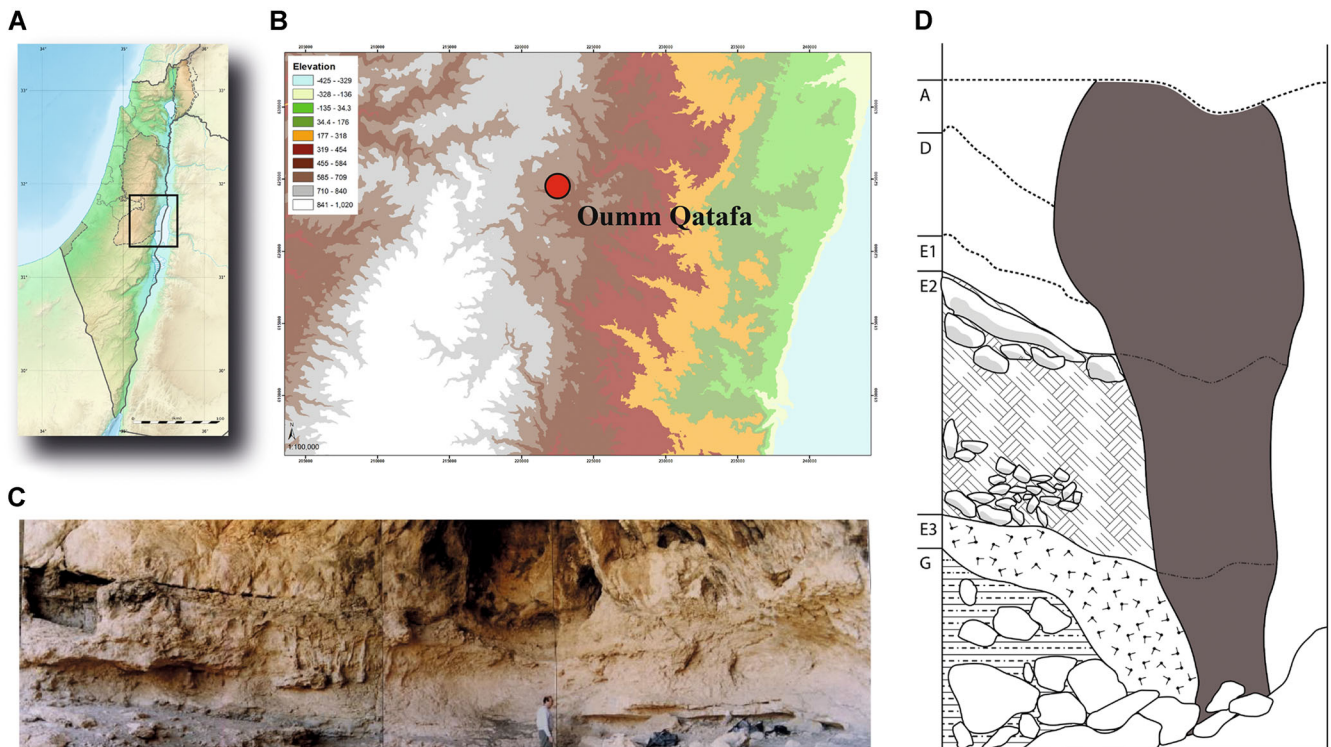


Figure 2. Location and site map for Oumm Qatafa: (A) panorama of the cave wall (courtesy of N. Porat); (B) location of the site in relation to local topography (map created by Ido Wachtel); (C) the region enlarged in B, modified from https://commons.wikimedia.org/wiki/File:Middle_East_topographic_map.png; (D) stratigraphic section of the cave (drawn by A. Marck based on Vaufrey 1931: Plate IV). [Color figure can be viewed at wileyonlinelibrary.com]

thick, respectively (Neuville 1951). Layer E1 was described as rich in fauna and was assigned to the Middle Acheulian based on the presence of amygdaloid-cordiform and lanceolate handaxes that occur in approximately similar frequencies (Bar-Yosef 1994; Gilead 1970; Neuville 1951).

Layer D2: This was a ~1 m thick layer, characterised by a light brown clay matrix. Based on handaxe typology, Neuville (1951), followed by Gilead (1970), proposed that this assemblage correlated with the Late Acheulian characterised by broad ovate, discoidal and cordiform bifaces. Layer D2 was dated by electron spin resonance (ESR) on herbivore tooth enamel to 213 ± 26 kya (Porat *et al.* 2002). More recently, three hominin phalanges found in this layer were analysed (using both morphometry and elemental analysis) to assess whether they were *in situ* or intrusive to this layer, i.e. derived from the overlying Layer A, dated to the Chalcolithic period (~6.5 kya) (Horwitz *et al.* 2011). The results do not negate the possibility that they are *in situ*.

Layer D1: A light brown clay matrix ~1 m thick, the lithic assemblage was identified as Micoquian Palaeolithic, i.e. terminal Acheulian with small bifaces and said to contain numerous bones. One U/Th series date for a stalagmite growing on top of the Acheulian layers gave an age of 115 000 BP, thus constraining the upper part of the Acheulian sequence in the cave (Porat *et al.* 1992).

Layer C: Sterile of archaeology, a clay matrix with brown limestone gravel and travertine, containing rodents.

Layer B: Sterile of archaeology, a clay matrix with brown limestone gravel, containing rodents.

Layer A: This layer was dated to the Chalcolithic period (4500–3800 BC) and yielded stone-lined dwelling pits, ceramics, flint artefacts, limestone and basalt ground stone artefacts, a fragment of an ossuary and Chalcolithic burials (Neuville and Boureau 1930; Neuville and Mallon 1931; Neuville 1951; Perrot 1992).

Materials and methods

Various palaeontologists analysed Neuville's fauna: Raymond Vaufrey (in Neuville 1931, 1951), who studied the macro-mammalian fauna while Georg Haas (in Neuville 1951) analysed the micromammals and reptiles. Subsequently, Eitan Tchernov (1962) examined the bird remains and later undertook a revision of the microfauna (Tchernov 1968, 1988).

The faunal remains from Oumm Qatafa are currently curated in the National Natural History Collections of the Hebrew University of Jerusalem. A few of the original remains that were recovered during excavations at the site and published by Vaufrey and Haas are missing. It is uncertain what happened to them, but it is assumed that these pieces were mislaid, together with most of the lithic assemblage, after being sent to the Institut de Paléontologie Humaine in Paris for analysis. The surviving pieces comprise most of those that were considered indicative by Vaufrey and appear in his 1931 and 1951 summary publications of the fauna from the site, and we therefore assume that they represent the taxonomic composition of the cave faunas at the presence/absence level.

A unique OQ number was given to each specimen we identified, and this is listed below by genus with the Layer (D1 to E3) to which it is attributed in parenthesis, based on the labels that were with the remains or the layer attributions for that specimen as published by Vaufrey (1931, 1951). We present the stratigraphic context in the tables below but do not use it in our analyses of the finds, which we treat as a single faunule of late Middle Pleistocene date *sensu lato*. This is justified by the fact that many of the finds, although fossilised and so not modern intrusions, did not have a layer attribution (missing labels). Moreover, aside from Layer D2, the precise dating of the different strata is unknown and has been extrapolated from dates for similar lithic assemblages at other Levantine sites. This approach enables us to accommodate

specimens that did not have contextual information as well as those which did.

Specimens were identified to taxon based on morphological comparisons with skeletal elements from the osteological collections of the Laboratory of Archaeozoology at the University of Haifa, the Laboratory of Palaeontology and Archaeozoology at the Hebrew University of Jerusalem, the mammal collection at the Museum für Naturkunde in Berlin, and relevant published literature. Some specimens could only be identified to higher taxonomic levels such as genus or tribe; we make the parsimonious assumption that such specimens represent the same population of identified species. Measurements (von den Driesch 1976) were taken to the nearest 0.1 mm using Mitutoyo dial calipers (SI1). For teeth, capital letters denote upper dentition, small letters mandibular teeth; deciduous teeth are noted by a lower case 'd' placed before the tooth type.

For rhinocerotids, we follow the nomenclature given in Pandolfi and Tagliacozzo (2015). Large bovids (notably *Bos* versus *Bison*) were identified using a suite of morphological and biometric criteria, as outlined in Horwitz and Monchot (2007). Size and dental morphology were used to resolve equid taxonomy (Davis 1980a; Eisenmann 1986). To facilitate identification based on enamel pattern, four equid teeth from the site (OQ 117, 118, 121, 998) had previously been sectioned by Davis and appear in his review article (Davis 1980a). In the current study, we benefited from non-invasive technologies and CT-scanned most of the teeth (OQ 113, 114, 115, 119, 120, 997, 998, 999) at the Laboratory for Bio-History and Evolutionary Medicine, Tel Aviv University. For other closely related taxa, such as caprines (*Ovis orientalis*, *Capra* spp.) and deer (*Dama* sp., *Cervus elaphus*), published morphological criteria were applied (e.g. Boessneck *et al.* 1964; Lister 1996; Prummel 1988; Zeder and Lapham 2010). The identification of a rare canid deciduous molar required detailed morphometric comparisons with museum specimens (for a list of the specimens, see SI2). These comparisons employed both linear (length, breadth) measurements and 2D geometric morphometrics, using 80 semi-sliding landmarks to capture the occlusal outlines, digitised with TPSdig (Rohlf 2017, ver. 2.31) and analysed using the 'geomorph' (Adams *et al.* 2021, ver. 3.3.2) package in R (see SI2 for data files and code). Herbivores and carnivores were also classified by size, following Brain (1983).

For pika, we collected the coordinates of 35 find spots of recent and subrecent *Ochotona rufescens* (Čermák *et al.* 2006; Khaki-Sahneh *et al.* 2014), a set of rasters representing current (1979–2013) climate based on standard 19 bioclim variables at 10 min resolution (Anthropocene, v1.2b: <https://chelsa-climate.org/>). These data were used to construct a maximum entropy model for the current distribution of the Afghan pika using the 'maxnet' package (Phillips 2021) in R (version 4.0.2; see SI3 for code and input files). Other libraries used include 'terra' (Hijmans 2021) and 'modEVA' (Barbosa *et al.* 2013). The model provided a list of variables that parsimoniously predict suitable environments for the Afghan pika, and also a projection of the probability of finding suitable habitats, as defined by the bioclimatic variables, in geographical space under present-day conditions. The values of the selected model bioclimatic variables at the present find spots were compared with the same values for Oumm Qatafa to examine its present climatic suitability as a habitat for pikas.

Age-at-death was quantified whenever possible using the state of epiphyseal fusion (Silver 1969) and tooth eruption and wear, using Payne's (1973, 1988) tooth wear stages for selenodonts. To increase sample size, we also described each tooth with a schematic wear stage: 'unworn', 'slight wear',

'active wear' and 'late wear', which was then used in conjunction with eruption time to place specimens in general 'young', 'adult' and 'old' categories. The same simplified scheme was also used for the few carnivoran dental remains. Hyrax teeth were assigned a wear stage and approximate chronological age following Fisher and Parkington (2020).

We recorded the completeness of specimens in order to calculate the minimum number of elements using the fracture summation approach (Klein and Cruz-Urbe 1984), but the small number of identified specimens in each taxonomic group and the dominance of dental fragments do not suggest any productive use of this statistic; number of identified specimens is therefore employed as the measure of quantification throughout. Bone-surface modifications, recorded by observing each specimen using a stereoscopic microscope at magnifications of $\times 5$ – $\times 20$, consisted of carnivore and rodent gnawing, cut marks, burning, weathering and abrasion. Bone end fractures were described as green, dry or mixed and the shaft circumference was given a percentage completeness score following Villa and Mahieu (1991). Bone size was measured along three dimensions (greatest length, greatest breadth and depth/thickness), and colour recorded as 'light', 'reddish', 'brown' and 'black'. Manganese staining was scored on a scale representing absence, sporadic spots, partial coverage and heavy staining. Since specimens in the last category could easily be mistaken for carbonised bones, Fourier transform infrared spectroscopy (FTIR) analyses were run on selected specimens to check our visual identification of burning (e.g. Lebon *et al.* 2009).

Ten samples that had been identified visually (based on colour) as probably burnt, were analysed by FTIR (Stiner *et al.* 1995). All samples were powdered and mixed with 5 mg of KBr. The mixture was pressed into a 7 mm die using a Pike hand press and analysed with a Thermo Nicolet iS5 FTIR spectrometer. FTIR spectra were collected by performing 32 scans with a resolution of 4 cm^{-1} in the $4000\text{--}400\text{ cm}^{-1}$ spectral range. The FTIR spectra were collected and baselined using *Omnice* software. The software was replotted using *OriginLab Pro* 2018 (b9.5.0193). The identification of burnt bones was performed by identifying the presence of a peak at 630 cm^{-1} in the infrared spectra attributed to hydroxylation of the bone mineral during exposure to heat above 600°C (Berna *et al.* 2012; Rey *et al.* 1995).

RESULTS

A total of 261 specimens were identified to taxon (Table 1). Of these, eight specimens derived from Layer F, 64 from Layer E, 62 from Layer D, and 127 could not be assigned to a layer. While 202 specimens could be assigned to the level of genus or species, some 59 specimens comprised bone and tooth fragments that could at best be assigned a body-size class. Without systematic recovery, the value of specimens unidentified to either taxonomic or skeletal element (Table 2) is very limited, and the latter group have been used here only for taphonomic analysis of bone surface modifications. Measurements for all specimens are given in a supplementary file (S1).

Systematic palaeontology

Order Perissodactyla Owen, 1848.

Family Rhinocerotidae Gray, 1821.

Genus *Stephanorhinus* Kretzoi, 1942.

Stephanorhinus hemitoechus (Falconer, 1859)

Referred specimens: OQ-259 (D2), left P3; OQ-260 (?D1), proximal radius.

Table 1. Taxonomic representation by layer, percentages rounded.

Taxon	Layer F		Layer E		Layer D		Unassigned		Total			
	NISP	%	NISP	%	NISP	%	NISP	%	NISP	%		
Perissodactyla	<i>Stephanorhinus hemitoechus</i>				1	2	1	1	2	1		
Artiodactyla	<i>Equus</i> spp.		2	20	4	7	3	5	11	7	21	7
	Cervidae											
	Cervidae gen. et sp. indet.				1	2	2	3	1	1	4	2
	<i>Cervus elaphus</i>				1	2	2	3	7	6	10	4
	<i>Dama dama</i>				5	8	5	8	16	13	26	10
	Bovidae											
	<i>Capra</i> sp.		2	20	7	11	22	35	30	24	61	23
	<i>Gazella</i> cf. <i>gazella</i>		2	20	2	3	7	11	14	11	25	10
	<i>Bos primigenius</i>				1	2	2	3	7	6	9	3
	Bovini gen. et sp. indet.						1	2			1	1
Hyracoidea	<i>Procavia capensis</i>		4	40	29		10	16	31	24	74	28
Lagomorpha	<i>Lepus capensis</i>						2	3	1	1	3	1
	<i>Ochotona</i> cf. <i>rufescens</i>				6		2	3			8	3
Carnivora	<i>Crocuta crocuta</i>				1		1	2	2	2	4	2
	<i>Canis</i> cf. <i>mosbachensis</i>				4		1	2	2	2	7	3
	<i>Vulpes vulpes</i>				2		1	2	4	3	7	3
	<i>Felis silvestris</i>				1				2	2	3	1
Total			10		64		62		129		265	
Richness (S)			3		12		14		15		17	

NISP: number of identified specimens.

Table 2. Skeletal element representation by size class in number of identified specimens.

Anatomical region		sz-1		sz-2		sz-3		sz-4		sz-5	
		E	D	E	D	E	D	E	D	E	D
Craniodental	mandibles	3	1	1	2	2	12	3	3		
Axis	maxillae	3	1		2	4	5	5	6		1
	carial			2	1	1	2		1		
	vertebrae				1		1	1			
	ribs										
Forelimb	pelvis										
	scapula										
	humerus						1		1		
Hindlimb	radius						1		2		
	ulna	1									
	femur				1		1		1		2
	tibia	1							3	1	
	astragalus										
Feet	calcaneus	1	2								
	metapodials							1			
	phalanx 1										
	phalanx 2										
	phalanx 3								1		

Taxonomic discussion: OQ-259 is an isolated left P3 that is highly worn, WS 7 on the scale of Taylor *et al.* (2013). In this stage of wear, the ectoloph, the protoloph and the metaloph are all fused (Fig. 3). The tooth is broken lingually, with parts of the hypocone and protocone not preserved. The premolar is highly molarised and the antecrochet is absent, which is the typical condition in *Stephanorhinus*. The crochet is simple but with slight folding; the crochet is typically simple in *S. etruscus*, simple or multiple in *S. hemitoechus*, and frequently multiple in *S. hundsheimensis* and in *S. kirchbergensis* (Guerin, 1980; Lacombat 2006). The crista is well developed but the medifossette is open; the presence of crista is more frequent in *S. hemitoechus* and *S. etruscus* than in *S. kirchbergensis* (Guerin, 1980; Lacombat 2006). The postfossette is large but

simple, with no enamel foldings. We note, however, that the morphology of some of these occlusal characters can be influenced by wear. The profile of the vestibular wall is irregular, with vertical folding. The paracone fold is moderately developed, like other specimens of *S. hemitoechus* and different from the more convex and less undulating outline of the ectoloph in *S. etruscus* and *S. kirchbergensis* (Guerin, 1980; Fortelius *et al.* 1993; Lacombat 2006). The labial enamel is rugose and there is some amount of cementum cover. OQ-259 is quite small (MD = 35 mm) but in this stage of wear it is compatible with *S. hemitoechus* (Van Asperen and Kahlke 2015). The upper premolars of *S. hemitoechus* usually have a metacone style (Fortelius *et al.* 1993) but this feature is not visible due to wear on OQ-259.



Figure 3. (A) *S. hemitoechus* OQ-259 (D2), P3; 1 – labial; 2 – occlusal; 3 – mesial; (B) *S. hemitoechus* OQ-260 (?D1), proximal radius; 1 – proximal; 2 – posterior; (C) *B. primigenius* OQ-255 (?), left astragalus; 1 – proximal; 2 – dorsal; 3 – lateral; 4 – plantar; (D) *B. primigenius*, OQ-256 (?), right distal scapula; 1 – lateral; 2 – medial; 3 – distal. (Photographs by Roeie Shafir). [Color figure can be viewed at wileyonlinelibrary.com]

A second rhinocerotid specimen from Oumm Qatafa, QQ-260, is a proximal radius fragment of a subadult individual (the fusion line is visible, and the size is rather small). The antero-posterior breadth is 42.8 mm while the medio-lateral width is ~74.9 mm. The specimen is scorched and its preservation state is poor with no diagnostic features on this specimen. We make a parsimonious assumption that both QQ-259 and QQ-260 belong to the same species.

The two rhinocerotid specimens were also identified by Vaufreycy (1931, 1951). He assigned them to Merck's rhinoceros *Rhinoceros mercki*, which is associated with woodland environments, although noting in 1931 that it resembled a rhino fourth premolar from Emireh Cave identified as *Dicerorhinus hemitoechus*, the steppe rhino (Garrod and Bate 1937). The similarity of the Oumm Qatafa specimen to that from Emireh Cave was accepted by Tchernov (1988: Table 10), who assigned the specimen to *D. hemitoechus* (currently *S. hemitoechus*),¹ though the reason for this reassignment was not made explicit.

Order Perissodactyla Owen, 1848

Family Equidae Gray, 1821.

Genus *Equus* Linnaeus, 1758.

The assemblage is small and most teeth are isolated finds, and either deciduous or juvenile. In consequence, very few determinations can be made with certainty even if, when possible, teeth were sectioned or scanned to highlight the enamel pattern. Moreover, fossil *Equus* are scarce for the Mid-Pleistocene, especially in the Levant, so that finding suitable comparisons is difficult. The following taxonomic descriptions represent a revision of those appearing online in Eisenmann.

Equus (*Quagga* Shortridge 1934) cf. *mauritanicus* Pomel 1897

Referred specimens: Vaufreycy (1931: Fig. 23) an upper right premolar (P4 or P3) and an upper left M1 (E); OQ-119 (D2/37),

upper left M1; OQ-117 (D2), lower left molar germ (Fig. 4, A–H). Upper cheek teeth have a size and enamel pattern similar to *E. mauritanicus* of Tighenif, Algeria (Eisenmann and Baylac 2000, Eisenmann 2000). On the lower cheek teeth, the ectoflexids are deep.

Taxonomic discussion: Vaufreycy (1951) attributed all equids in the Oumm Qatafa assemblage (Layers E3, E2–1 and D2) to *Equus* cf. *mauritanicus* – the fossil North African quagga. This attribution was based on the size and morphological resemblance of upper cheek teeth to North African specimens of this taxon. Unfortunately the permanent upper cheek teeth from Layer E that were identified by Vaufreycy are not in our collection. However, the two equid fossils from this layer that have survived are too large for *E. mauritanicus*, except for OQ-116, a small upper left decidual incisor from Layer E2/3, which, as described below, we have attributed to *E. hydruntinus* (Supplement Fig. B).

Furthermore, the additional specimen attributions of Vaufreycy (1951) to *E. mauritanicus* are difficult to discuss since most of them concern fossils from Layer D2 that are not present in the current collection that comprise: two metapodials (distal breadth 39 mm), a first phalanx (length 70 mm), a distal radius and tibia, both slightly larger but corresponding to another Algerian example (Cave of Alain), an astragalus considered by Vaufreycy to derive from an especially large individual of this species, and an incomplete atlas vertebra. In the case of the metapodial we have additional information since Vaufreycy (1951) noted that the dimensions of the two Layer D2 metapodials correspond perfectly to a Mousterian *Equus* cf. *mauritanicus* specimen from Ain Metherchem in Tunisia. In the IPH collections in Paris there is a small and slender metacarpal from the Aterian of Ain Metherchem, Tunisia (Aouadi *et al.* 2014), measuring 39.5 mm in distal breadth. The Simpson's diagram (Suppl. Fig. C) shows that any reference to *E. mauritanicus* would be wrong; the MC from Ain Metherchem belonged to an ass and thus so do the metapodials of Oumm Qatafa D2 since, according to Vaufreycy, they corresponded perfectly to the Tunisian specimen.

¹For nomenclature we follow Pandolfi (2018).

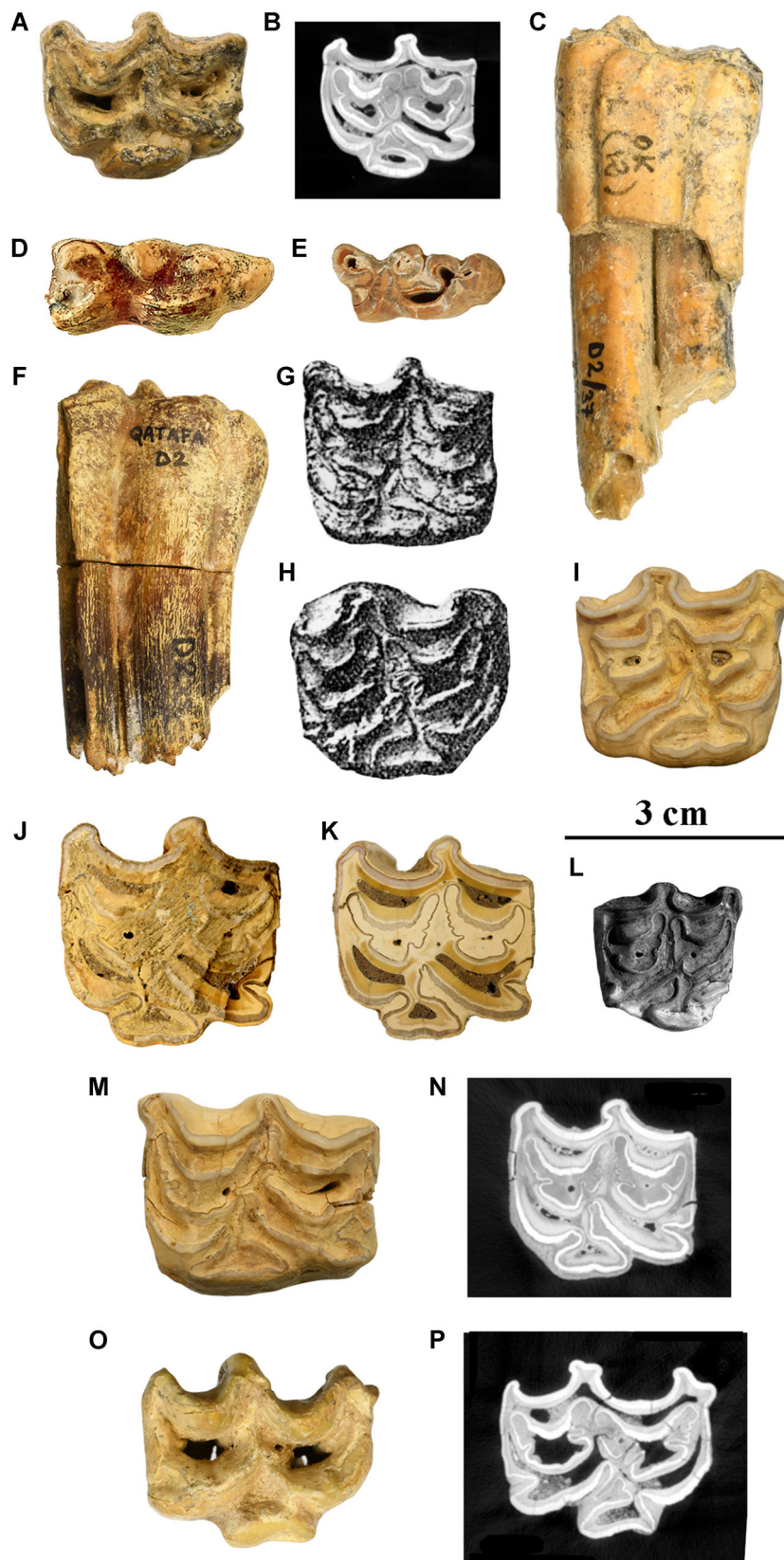


Figure 4. (A, B, C) *E. cf. mauritanicus*, OQ-119 (Layer D2), upper left molar, A: occlusal view, B: section, C: lingual view. (D, E, F) *E. cf. mauritanicus*, OQ-117 (Layer D2), lower left molar, D: occlusal view, E: CT-scan, F: vestibular view. (G, H): *E. cf. mauritanicus*, from Vaufrey 1931: Fig. 23, (Layer D1), G: upper left molar, H: upper right premolar. (I): *E. melkiensis*, OQ-999 (layer unknown), upper right premolar. (J, K): *E. aff. africanus*, OQ-121 (Layer D2), upper left molar, J: occlusal view, K: section. L: *E. hydruntinus*, OQ-120 (Layer D2), upper right molar. (M, N): *E. aff. africanus*, OQ-998 (layer unknown), upper left molar, M: occlusal view, N: scan. (O, P): *E. ferus*, OQ-997 (layer unknown), upper right premolar, O: occlusal view, P: scan. (Photographs by Roeie Shafir and Vera Eisenmann). [Color figure can be viewed at wileyonlinelibrary.com]

Equus (*Quagga* Shortridge, 1934) *aff. capensis* Broom 1909

Referred specimens: With some doubt: OQ-122 (E2), left distal tibia; OQ-123, (E2), left calcaneus; OQ-124 (E2), left talus; OQ-125 (?), first phalanx (Supplement Fig. A).

With even more doubt: OQ-113 (E1) right lower deciduous premolar; OQ-114 (E1), right upper deciduous premolar; OQ-115 (E1), left upper deciduous premolar (see Supplement Figs A and B).

Taxonomic discussion: As part of his revision of equid taxonomy for Israeli sites, Davis (1980a) re-examined the

equid remains from Oumm Qatafa and concluded that equids of two different sizes were present at the site; a small equid, *E. hydruntinus*, and a large equid identified as *E. cf. caballus* – based on a complete talus bone (Davis 1980a: Fig. 14), while Vaufrey (1931) had noted that the equid remains from Layer E do not fit a true *E. caballus*. Caballines and Quaggas both have rather large and robust limb bones that are very difficult to differentiate. But the quagga's tali usually have relatively narrower distal articulations like the Oumm Qatafa specimen.

The Oumm Qatafa talus is similar by size and proportions (see Supplement S11) to specimens from the early Middle Pleistocene site of Gomboré II (Melka Kunturé, Ethiopia) and has the dimensions of the average *E. capensis* of Elandsfontein (Eisenmann 2000, 2014), but it is quite a lot larger than *E. mauritanicus*, as is the first phalanx. We have no data on the limb bones of the large *Equus* from Olorgesailie Formation (Kenya) from levels dating to ~1 Ma years old (Potts *et al.* 2018) that was recently referred to *E. oldowayensis* (Bernor *et al.* 2019), but it is probably of the same size.

Equus (*Asinus* Gray, 1824) *melkiensis*, Bagtache, *et al.* 1984.

Referred specimen: OQ-999 (?) upper left P3 or P4 (Fig. 4, I).

Taxonomic discussion: An upper premolar from Oumm Qatafa has the typical morphology of *E. melkiensis*, an Algerian Aterian species; a plump, symmetric bilobed protocone, moderate enamel plication, deep post-protoconal groove but presence of a pli caballin (caballine fold). Similar patterns are known earlier in specimens from Sidi Abderrahman, Morocco (at the top of DO; Eisenmann 2020) but also from the Israeli sites of Gesher Benot Ya'akov (Eisenmann 2006, 2012b) and tentatively also Nahal Hesi (Yeshurun *et al.* 2011), in Yemen (specimens of unknown age and location; Eisenmann 2006) and in Tajikistan (Lakhuti II, just below the Bruhhes-Matuyama boundary; Eisenmann 2006). The origin and direction of a possible dispersion (if the resemblances are not purely due to homoplasy) is naturally a matter of conjecture, but Tajikistan does seem the place of the earliest occurrence of this equid form. Recently, a suggestion has been made that this extinct taxon contributed to domestic ass lineages (Sam 2020). In North Africa, *E. melkiensis* succeeds the asinine *Equus tabeti*. The same may also be true for the southern Levant, since *E. tabeti* is documented in Early Pleistocene 'Ubeidiya and perhaps the Daqara Formation (Scardia *et al.* 2019) as well as in and the early Middle Pleistocene site of Evron Quarry (near the Brunhes–Matuyama transition of 0.77 Ma, Shemer *et al.* 2019), while *E. melkiensis* has been definitely identified at the sites of Gesher Benot Ya'akov (~0.78 Ma) and Oumm Qatafa.

Equus (*Asinus* Gray 1824) aff. *africanus* Heuglin *et* Fitzinger 1866

Referred specimens: OQ-121 (D2) upper left P4; OQ-998 (?), upper left M1 or M2 (Fig. 4, J, K, M, N); in addition, two metapodials are mentioned by Vaufrey (1951) as derived from Layer D2.

Taxonomic discussion: In North Africa there are numerous forms that present ass-like characteristics in the enamel pattern of cheek teeth and the proportions of limb bones but do not quite resemble *E. africanus* nor *E. melkiensis*. In particular, they have deeper diaphyses on the metapodials like the specimens mentioned by Vaufrey. The Oumm Qatafa specimens resemble this group of asinines.

Equus (*Hemionus* Pallas 1775) *hydruntinus* Regalia 1907

Referred specimens: OQ-120, (D2), upper right M2; OQ-116 (E2/3), upper left dl (Fig. 4L).

Taxonomic discussion: Previously Eisenman (1992, 2012a) concurred with Davis (1980a) that several fossils from Oumm Qatafa probably belong to a smaller equid, *E. hydruntinus*, a form related to modern hemiones (Eisenmann 2006). It seems now that there are only two certain attributions: an upper right M2 (Fig. 4, L) and an upper left dl (Supplement 6 Fig. B). The other previous attributions to this species, made on fragments and/or decidual specimens that are not particularly small, were reconsidered and rejected by us.

We assign the two identified specimens to the smaller equid *E. hydruntinus* that has been identified at Late Mid-Pleistocene sites in the southern Levant (e.g. Yabrud I, Oumm Zinat, Azraq

Spring C, see Horwitz and Chazan 2007: Table 13.4 and references therein) and is especially common in even later Mid-Pleistocene to Late Pleistocene contexts such as Tabun, Kebara, Qafzeh and Qesem (Davis 1977; Stiner *et al.* 2009).

Equus (*Equus* Linnaeus 1758) *ferus* Boddaert 1785

Referred specimen: OQ-997, (?), upper right premolar. (Fig. 4, O, P). The section (Fig. 4, P) evidences the grooves on parastyle and mesostyle usual in Caballines.

Taxonomic discussion: *E. ferus* is the dominant equid species in the assemblage from Tabun E (Eisenmann 1992) and Qesem Cave (Stiner *et al.* 2009), both roughly contemporaneous with levels at Oumm Qatafa. Caballine equids have also been identified at the early Middle Pleistocene site of Gesher Benot Ya'akov (Eisenmann 2006).

Genus *Equus* Linnaeus, 1758.

Equus sp.

Referred specimens: OQ-161 (E1/7), a cervical vertebra; OQ-171 (?), upper prefossette; OQ-231 (?), tibia diaphysis fragment; OQ-232 (?), right tibia diaphysis fragment; OQ-242 (?), tibia diaphysis fragment; OQ-257 (D2), right upper molariform tooth fragment.

Taxonomic discussion: These remains could not be attributed to a specific equid species.

Order Artiodactyla Owen, 1848.

Family Bovidae Gray, 1821.

Tribe Bovini, Gray 1821.

Genus *Bos* Linnaeus, 1758.

Bos primigenius Bojanus, 1827.

Referred specimens: OQ-51 (?), left distal femur (D2); OQ-58 (?), subadult second phalanx; OQ-62 (E1), left distal tibia; OQ-144 (?), right distal ulna; OQ-163, unerupted right M1 (D2); OQ-233 (?), left tibia shaft; OQ-235 (?), tibia diaphyseal fragment; OQ-243 (?), distal femur; OQ-255 (?), right astragalus; OQ-256 (?), right distal scapula.

Taxonomic discussion: Vaufrey (1951) identified remains of a large bovid in Layers D2 and D1, that he ascribed to *Bos* or *Bison*. No large bovid remains were noted by him from any of the other layers. We have attributed nine remains to *Bos*, one each from layers E1 and D2, the remainder from unknown levels. Although it is difficult to attribute isolated and often fragmentary remains of Bovinae, the observed morphology conforms more closely to *Bos* than *Bison*. For example, OQ-255, a right astragalus that is lightly weathered (GLI = 87.6 mm, Bd = 58.4 mm, DI = 47.0 mm), has a squat and robust form rather than being elongated and slender as in *Bison* (Stampfli 1963) (Fig. 3). This is manifest in the length/distal breadth index, which gives a value of 66.6, placing the piece within the *Bos* range (≥ 58 mm) rather than in the lower range characteristic of *Bison* (≤ 58 mm). Moreover, the depression on the cranial aspect of the bone, between the plantar and distal trochlea, forms a right angle as is typical of *Bos*, rather than an obtuse angle as in *Bison*.

Bovini gen et sp. indet.

Referred specimens: OQ-19 (D2), upper second or third molar.

Taxonomic discussion: Specimen OQ-19 is a mesial fragment of a highly worn upper second or third molar (Fig. 5). This tooth was identified by Vaufrey (1951) as a large antelope, but in our view belongs to a bovine, probably a small *Bos primigenius* (L = 16.1 mm, B = 12.1 mm). The most interesting feature is the large, square-shaped entostyle. However, the size and shape of bovid molar entostyles can vary quite ostensibly with wear: the base tends to be wider and to have more vertical angles as wear progresses.

Genus *Capra* Linnaeus, 1758.

Capra cf. *ibex* Linnaeus, 1758.

Referred specimens: OQ-3 (?), left distal humerus; OQ-5 (D2), left M2; OQ-6a (F), upper molar fragment; OQ-7 (E2),

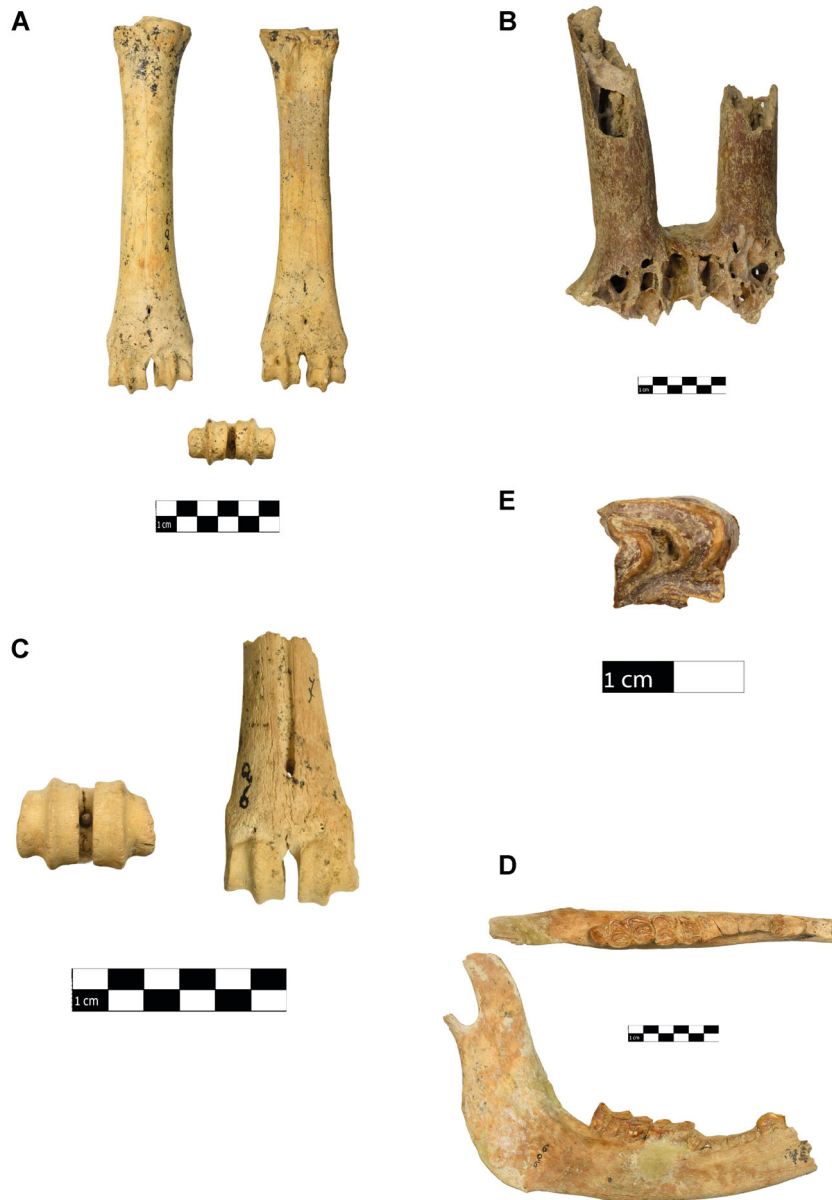


Figure 5. (A) *Capra cf. ibex* OQ-201 (?), complete right metacarpus; (B) *Capra cf. ibex* OQ-230 (E2), cranium fragment with horn cores; (C) *Dama* sp. OQ-41 (?), left distal metatarsus; (D) *Cervus elaphus* OQ-221 (?), right dp3-m3. (E) *Bovini* gen. et sp. indet., OQ-19 (D2), upper second or third molar. (Photographs by Roeie Shafir). [Color figure can be viewed at wileyonlinelibrary.com]

right M1; OQ-10 (E1), right m3; OQ-11 (?), right P3; OQ-12 (D2), right m3; OQ-15 (D2), incisor; OQ-16 (D2), incisor; OQ-21, isolated right P4; OQ-23a (D2), left M2; OQ-25 (D2), left M2; OQ-28 (?), incisor; OQ-30 (E1), left p3; OQ-33 (D2), left p4; OQ-34 (D2), right dp3; OQ-35 (E2), right M3; OQ-36 (D2), right M3; OQ-53 (?), distal left metacarpus; OQ-57 (?), proximal left metacarpus; OQ-83 (?), right m2; OQ-97 (?), thoracic vertebra corpus; OQ-128 (E1), left P2-M1; OQ-130 (E1), left M2; OQ-131 (D2), incisor; OQ-132 (D2), incisor; OQ-133 (D2), incisor; OQ-148 (?), molar fragment; OQ-150 (D2), right horn core fragment; OQ-152 (D2), left m3; OQ-154 (D2), right distal humerus; OQ-156 (F), isolated left M3; OQ-164 (D2), isolated right M3; OQ-166 (D2), right m3; OQ-167 (?), right calcaneus; OQ-172 (?), horncore fragment; OQ-189 (?), molar fragment; OQ-190 (?), upper fragment; OQ-191 (?), molar fragment; OQ-192 (?), isolated M fragment; OQ-193 (?), molar fragment; OQ-196 (D2), right proximal radius; OQ-198 (D2), horncore fragment; OQ-201 (?), complete right metacarpus; OQ-202 (?), right metacarpus, unfused, distal epiphysis missing; OQ-203 (?), left proximal ulna; OQ-204 (?), left distal humerus; OQ-205 (D2), left p4-m3; OQ-206 (?), left p3-m3; OQ-207 (D2), right m1-m3; OQ-208 (?), right P3-M2; OQ-209 (?), right m3; OQ-210 (?), right m3; OQ-211 (?), left m3; OQ-212 (?), left M3; OQ-213 (?), right m2; OQ-214 (?), right M3;

OQ-215 (?), left M3; OQ-216 (?), right m3; OQ-230 (E2), cranium fragment with horn cores; OQ-258 (D2), left m2.

Taxonomic discussion: *Capra* occurred in all layers of the site and were attributed by Vaufrey (1931, 1951) to *Capra ibex*, an identification upheld by Tchernov (1988). We identified 61 remains to *Capra* which comprise the largest number of identified bones in the assemblage (Fig. 5). This includes bones and teeth from Layers F ($n=2$), E1 ($n=7$), D2 ($n=22$), and also unassigned specimens ($n=31$).

During the Pleistocene, two species of the genus *Capra* are known from the region; the Nubian ibex (*Capra ibex nubiana*) and the larger bezoar wild goat (*C. aegagrus*): 101 cm body length, 70 cm withers height and 50–60 kg versus 150 cm total length, 95 cm withers height and 70–80 kg, respectively (Heptner *et al.* 1988; Uerpman 1987). The larger ibex and bezoar goats may overlap in size, especially between adult females and juvenile males. Moreover, post-cranial remains of the two taxa are not readily distinguishable and they are also too fragmentary to attempt species separation at Oumm Qatafa. The ibex and bezoar goat can, however, be distinguished by their horn cores, of which one base has been found at the site (OQ-230); it has a weak posterior keel suggesting that it belonged to the Nubian ibex. Notably, none of the remains from the site conform to *Ovis* based on

Table 3. Capra tooth eruption and wear.

Layer	Element	Teeth	Observation	Estimated age-at-death
Layer E	mandible	P3	active wear	adult
	mandible	M3	TWS C	adult
	maxilla	P2,P3,P4,M1	P4 in	adult
	maxilla	M3	active wear	adult
Layer D	maxilla	M1	early wear	adult
	maxilla	M1	active wear	adult
	mandible	M1,M2,M3	TWS G	adult
	mandible	P4,M1,M2,M3	TWS E	adult
	mandible	M3	active wear	adult
	mandible	P4	TWS E	adult
	mandible	dp3	TWS A–B	young
	maxilla	M3	late wear	old
	maxilla	M2	active wear	adult
	maxilla	M2	active wear	adult
	maxilla	M2	active wear	adult
maxilla	M3	active wear	adult	

TWS: tooth wear stage (following Payne 1973).

morphological criteria (e.g. Boessneck *et al.* 1964; Halstead *et al.* 2002; Zeder and Lapham 2010).

The ecotonal position of the site, in the region of biogeographical overlap between the two taxa (Uerpmann 1987), makes any taxonomic assumption based on habitat preference very uncertain although ibex currently inhabits the Judean Desert (Mendelssohn and Yom-Tov 1999). It was suggested by Uerpmann (1987: 116) that these sympatric *Capra* species could have shared the same region utilising topographical and altitudinal habitat gradients. In most publications on Middle Pleistocene Levantine sites, the species of goat is not noted. Exceptions include the identification of *C. aegagrus* recorded as present at Masloukh and Tabun E based on biogeographical arguments, while *C. ibex* is listed as present at Yabroud I and Zuttiyeh in addition to Oumm Qatafa on the same grounds (Horwitz and Chazan 2007).

Tooth eruption and wear observations (Table 3) suggest that most of the Oumm Qatafa caprines that could be assigned an age class were adults ($n = 13$), with only one juvenile and one senescent individual found in Layer D.

Genus *Gazella* Blainville, 1816

Gazella cf. gazella (Pallas, 1766)

Referred specimens: OQ-3 (?), left proximal metatarsus; OQ-13 (D2), left DP2; OQ-22 (E1), horncore, female; OQ-29 (F), right m2; OQ-32 (E1), incisor; OQ-60, left distal humerus; OQ-84 (?), left humerus shaft and distal fragment; OQ-134 (D2), deciduous incisor; OQ-135 (D2), incisor; OQ-136 (D2), DP2; OQ-151 (D2), thoracic vertebra; OQ-165 (F2), left distal tibia; OQ-183 (?), dp3-dp4-m1; OQ-187 (?), left hemimandible with dp3-m1; OQ-199 (D2), horncore, male; OQ-200 (D2), left distal femur; OQ-245 (?), left distal metatarsus; OQ-247 (?), left proximal metatarsus; OQ-248 (?), proximal metatarsus; OQ-249 (?), right distal metacarpus; OQ-250 (?), right distal tibia; OQ-251 (?), distal tibia; OQ-252 (?), left distal humerus; OQ-253 (?), distal humerus fragment; OQ-254 (?), left horncore.

Taxonomic discussion: Vaufrey (1951) identified only nine remains of gazelle at the site, and these were not attributed to species, but listed by him as *Gazella* sp. These consist of a single bone from Layer E3 and eight specimens from Layers D2 and D1, comprising two mandibles with deciduous teeth, humerus, radius, metacarpal (Layer D1), metatarsal, astragalus, calcaneum, first phalange (posterior) (Layer D2). In contrast to Vaufrey, we have identified 24 specimens as belonging to gazelle, of which 10 have layer attributions.

Three gazelle taxa are currently recognised in Israel which differ in their biogeography (Mendelssohn and Yom-Tov 1999). The most ubiquitous is the mountain gazelle *Gazella gazella*, that inhabits the Mediterranean region; an endemic subspecies, the Acacia gazelle *G. gazella acaciae*, is found in a restricted part of the southern Arava; and the dorcas gazelle, *Gazella dorcas*, occurs throughout the Negev and Judean Desert. They exhibit interspecific differences in body size and horn morphology (Davis 1980b; Mendelssohn and Yom-Tov 1999; von den Driesch and Boessneck 1995: 89). Today, Oumm Qatafa lies in the region of overlap of both the mountain and dorcas gazelle range, making species identification challenging. The measurements of specimens from Oumm Qatafa, however, plot within the higher part of both the male and female range of modern *G. gazella* (Fig. 6), suggesting that an attribution to this gazelle species is more likely than to the smaller *G. dorcas*. *Gazella* remains are present, but not common, at the Early to Mid-Pleistocene sites of 'Ubeidya, Geshen Benot Ya'akov, Bizat Ruhama, Nahal Hesi and Evron Quarry (Martínez-Navarro *et al.* 2012; Rabinovich and Biton 2011; Yeshurun *et al.* 2011), although the subspecies assignment to *G. gazella* is in most cases tentative. Gazelle remains increase in frequency in the latermost Mid-Pleistocene to Late Pleistocene sites such as Bezez I, Tabun, Zuttiyeh, Revadim and Qesem Cave, where the presence of mountain gazelle has been validated based on both morphological and metrical grounds (Horwitz and Monchot 2007; Stiner *et al.* 2009).

Family Cervidae Goldfuss, 1820

Genus *Cervus* Linnaeus, 1758

Cervus elaphus Linnaeus, 1758

Referred specimens: OQ-14 (D2), incisor; OQ-54 (?), left proximal ulna; OQ-59 (?), ulnar fragment; OQ-126 (D2), third phalanx; OQ-149 (E1), distal metacarpal; OQ-158 (?), right P4; OQ-217 (?), right proximal metatarsus; OQ-218 (?), left proximal metatarsus; OQ-219 (?), left proximal metatarsus; OQ-221 (?), right dp3-m3.

Taxonomic discussion: Vaufrey (1931) lists a complete metatarsal (length = 290 mm), which he attributes to *Cervus elaphus* rather than *Dama* based on its size and morphology. The bone is very asymmetrical due to an exaggerated swelling of the half of the shaft on the anterior aspect (but not as if the two sides had slipped one over the other which is a characteristic of *Dama*). Vaufrey also attributed a right mandible to *C. elaphus*. This jaw (OQ-221) (Fig. 5) is extremely large with heavy wear of the premolars into the dentine, in addition to some upper teeth and several metapodials. His identification was based on premolar morphology, which in *Cervus* are more molarised than those of *Dama*. This molarisation, which includes the development of the larger second lobe, is attested in the Oumm Qatafa specimen despite its extreme wear.

Additional finds that we attribute to *C. elaphus* (some are not noted by Vaufrey), are OQ-149 (E), distal metatarsal (Dd = 30.1 mm), which is within the size range of European *C. elaphus* specimens (di Stefano *et al.* 2015: 118); OQ-158, a P4 (L = 16.2 mm, B = 20.7 mm); and OQ-54, a proximal ulna; possibly paired metatarsal fragments, both consisting of the proximal articulation and much of the shaft (OQ-217 right and OQ-218 left); OQ-219, another proximal metatarsal fragment.

Genus *Dama* Frisch, 1775

Dama dama cf. mesopotamica (Brooke, 1975)

Referred specimens: OQ-1 (?), left distal tibia; OQ-2 (?), left tibia diaphysis; OQ-6 (D2), left distal tibia; OQ-9 (E2), left dp4; OQ-24 (D2), left M1; OQ-31 (E1), right dp3; OQ-38 (?), left m1-m2; OQ-39 (?), left dp4-m1; OQ-40, first phalanx; OQ-41 (?), left distal metatarsus; OQ-42 (?), left distal metatarsus; OQ-43 (?),

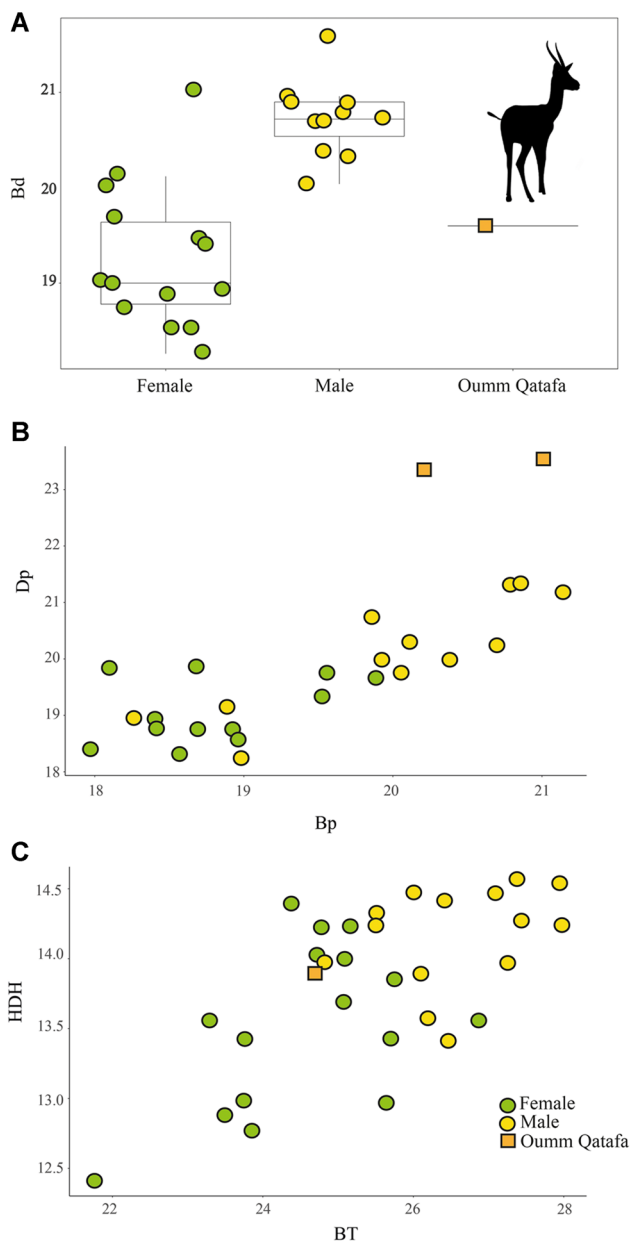


Figure 6. Gazelle metacarpus (A), metatarsus (B) and humerus (C) measurements plotted with recent male and female *Gazella gazella* from Israel (measurements from Horwitz *et al.* 1980). [Color figure can be viewed at wileyonlinelibrary.com]

right distal metatarsus; OQ-44 (?), right proximal metatarsus; OQ-45 (?), left proximal metatarsus; OQ-52 (?), right proximal radius; OQ-56 (?), right distal metatarsus; OQ-127 (E2), right distal tibia; OQ-129 (E2), left M3; OQ-153 (D2), left dp4-m1; OQ-157 (?), left dp2-dp4; OQ-162 (E1), distal metapodial fragment; OQ-180 (?), second phalanx; OQ-220 (?), left distal metatarsus; OQ-223 (D2), right proximal radius; OQ-37 (?), left distal humerus; OQ-244 (D2), left proximal radius.

Taxonomic discussion: Remains of *Dama* were reported by Vaufreycy (1931, 1951) from all layers at the site, but were noted by him as being less frequent than those of *Cervus*. He listed a part of the mandible with three molars, which fits the size for this species (length = 65 mm), another mandible with three molars (deciduous teeth) from Layer D1 (tooth row length = 41.5 mm), an occipital bone, distal humerus (Layer E3, breadth = 47 mm), proximal radius, distal tibia, a navicular-cuboid, a metacarpal and five metatarsals (one complete; length = 23.8 mm) (Fig. 5).

Family Cervidae Goldfuss, 1820

Gen. et sp. indet.

Referred specimens: OQ-8 (E2), right upper molar; OQ-17 (D2), molariform tooth fragment; OQ-55, first phalanx; OQ-197 (D2), petrosium.

Taxonomic discussion: These remains were too fragmentary to be attributed to a specific cervid species.

Both *Cervus* and *Dama* are recorded in the early Middle Pleistocene sites of Evron Quarry and Gesher Benot Ya'akov (Tchernov 1988). At the latter site, the presence of numerous and consistent cut, chop and percussion marks on remains of *Dama* led Rabinovich *et al.* (2008) to argue that they represent one of the earliest examples of methodological butchering strategies. Remains of both cervid species, especially *Dama*, are even more frequent at the latest Mid-Pleistocene to Late Pleistocene Levantine sites (Garrod and Bate 1937; Horwitz and Chazan 2007) and dominate assemblages, as at Qesem Cave (Stiner *et al.* 2009).

Order Hyracoidea Huxley, 1869

Family Procaviidae

Genus *Procavia*

Procavia capensis Pallas, 1766

Referred specimens: OQ-63 (F2), left maxilla with M1-M3; OQ-64 (D2), right P4 germ; OQ-65 (F2), left I1; OQ-66 (F2), fragment of I1; OQ-67 (F2), left hemimandible with m1-m2; OQ-69 (E1), left P4 germ; OQ-70 (E1), left P3 germ; OQ-71 (E1), right p4 germ; OQ-72 (E1), left p4 germ; OQ-73 (E1), left p4 germ; OQ-74 (?), left ulna; OQ-74a (E1), left calcaneum; OQ-90 (?), right I1; OQ-91 (?), right I1; OQ-92 (?), right hemimandible with p4-m2; OQ-93 (?), right hemimandible with m2; OQ-94 (?), mandibular fragment with dp3 or dp4; OQ-95 (?), left mandibular fragment; OQ-96 (?), fragment of mandibular symphysis; OQ-101 (?), left distal tibia; OQ-105 (E1), left proximal ulna; OQ-143 (?), left incisor; OQ-179 (?), fragments of I1; OQ-261 (?), left proximal femur; OQ-262 (?), right distal femur; OQ-263 (?), right radius; OQ-264 (?), right distal ulna; OQ-265 (D2), right hemimandible with p3-m3; OQ-266 (?), left hemimandible with p2-m3; OQ-267 (?), right hemimandible with p4-m1; OQ-268 (?), maxillary incisor; OQ-269 (?), maxillary incisor; OQ-270 (?), right maxilla with P1-M2; OQ-271 (D2), left maxilla with P4-M3; OQ-272 (?), left maxilla with P1-M2; OQ-273 (E1), left hemimandible with dp2-dp3; OQ-274 (E1), left P4; OQ-275 (E1), left dP3; OQ-276 (D2), right P2-P3; OQ-277 (?), left m2; OQ-278 (E2), right deciduous maxillary premolar; OQ-279 (?), maxillary fragment; OQ-280 (?), left p4; OQ-281 (?), right p3; OQ-282 (E1), right P4; OQ-283 (E1), left P3; OQ-285 (E1), right p4; OQ-286 (?), right I1; OQ-287 (D2), left P1; OQ-288 (D2), left dP1; OQ-289 (D2), left dP1; OQ-290 (D2), right dP3; OQ-291 (D2), left dP3; OQ-292 (D2), left P2; OQ-293 (E1), right M3; OQ-294 (E1), right m2; OQ-295 (E), right P3 germ; OQ-296 (E1), left dp4; OQ-297 (E1), right P2 germ; OQ-298 (E1), right dp; OQ-299 (E1), left P4 germ; OQ-300 (E1), left P4; OQ-301 (?), left dp4; OQ-302 (E1), left p3; OQ-303 (E1), left P3 germ; OQ-304 (E1), left P3 germ; OQ-305 (E1), maxillary molariform germ; OQ-306 (E1), right p2; OQ-307 (E1), mandibular molariform germ; OQ-381 (?), left pelvic fragment; OQ-386 (?), left pelvic fragment; OQ-388 (?), left distal humerus; OQ-389 (?), right humerus; OQ-390 (?), right ulna.

Taxonomic discussion: According to Vaufreycy (1951), *Procavia* is present from Layer E3 to Layer D2. The collection of *Procavia capensis* identified by us, contains 74 bones and teeth from Layers F ($n=4$), E1 ($n=29$), D2 ($n=10$), and also numerous specimens unassigned to layers ($n=31$). Hyrax body-size gradients follow Bergmann's rule and have been used to track climatic changes in the Pleistocene record (Klein and Cruz-Urbe 1996). A comparison of tooth measurements

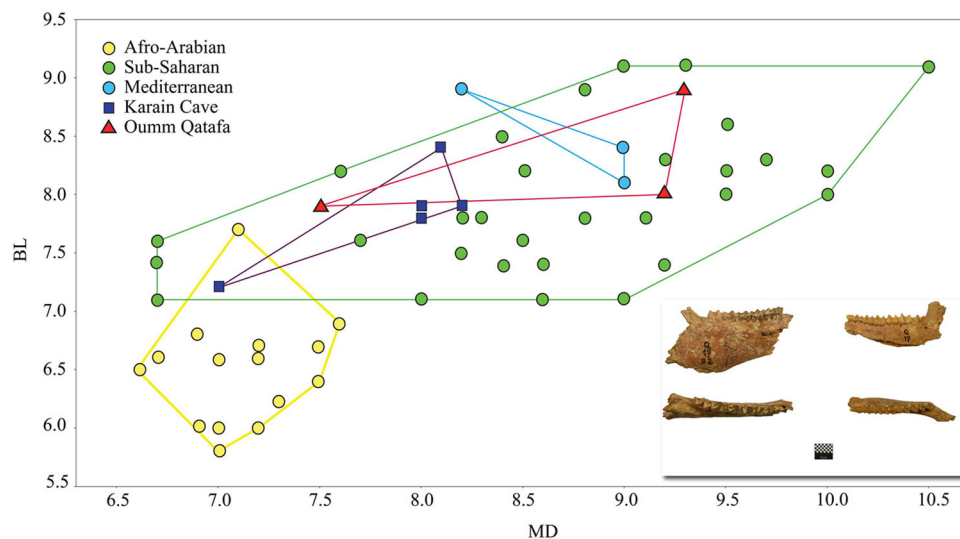


Figure 7. Hyrax dental breadth and length measurements from Oumm Qatafa compared with other recent and palaeontological groups. [Color figure can be viewed at wileyonlinelibrary.com]

Table 4. *Procapra* tooth eruption and wear, following Fisher and Parkington (2020).

Layer	Element	Teeth	Observation	Estimated age-at-death
Layer E	mandible	dp	deciduous	young
	mandible	dp	deciduous	young
	mandible	dp	deciduous	young
	maxilla	dp	deciduous	young
	maxilla	dp	deciduous	young
	maxilla	P2	erupted	juvenile
Layers D1 & D2	maxilla	P4,M1,M2,M3	P4(E4), M1(E4), M2(E3), M3 (E2), (early year 3)	adult
	mandible	P3,P4,M1,M2,M3	M1(E2), M2(E2), M3(E1)(year 3)	old

from OQ (S11) with recent and Pleistocene measurements (Fig. 7) indicate that the Oumm Qatafa hyrax were larger than their recent Saharo-Arabian conspecifics; they resemble both recent sub-Saharan and the Pleistocene hyrax from Qarain Cave (southern Turkey), which in turn are even larger. The hyrax dental remains from Layer E for which age-at-death could be determined were very young ($n = 5$ with deciduous dentition), and only one was a juvenile, with an erupted, but yet unworn, P2 (Table 4). Fewer but more accurate age estimations could be obtained from adult tooth rows ($n = 2$) from Layer D, which belonged to an adult that died at the age of three, and an older individual that died at the end of the third year of life.

Order Lagomorpha Brand, 1855

Family Leporidae

Genus *Lepus*

Lepus capensis Linnaeus, 1758

Referred specimens: OQ-100 (?), left distal humerus; OQ-106 (D2), right calcaneus; OQ-107 (D2) left calcaneus.

Taxonomic discussion: Three specimens of a medium-sized lagomorph were attributed to the Cape hare, *Lepus capensis*. Two of them derive from Layer D2: OQ-106 and OQ-107. Both are calcanei, the first unfused (greatest length (GL) = 25.7 mm), and the second fused (GL = 27.3 mm). A fused distal humerus OQ-100 (Bd = 11 mm; HTC = 6.5 mm) cannot be assigned to a layer. Vaufreij (1951) listed only two calcanea as belonging to *Lepus* (lengths 0.27 and 0.28 cm, respectively), both from Layer D2. He identified them as belonging to a small lagomorph which he termed *Lepus [europeus] syriacus*, a subspecies of the brown hare that is found in Turkey, Syria and Lebanon (Demirbaş and Albayrak 2014). Here we follow Yom-

Tov (1967) and Mendelssohn and Yom-Tov (1999) who designated the hare in Israel as belonging to the Cape hare, *Lepus capensis*, although microsatellite studies have suggested to split this population into brown hare in northern Israel and Cape hare in the south (Suchentrunk *et al.* 2000). Recent genetic analysis suggests that African Cape hare and brown hare may in fact be connected via gene flow, with Israel being a transitional zone with intergrading populations (Ben Slimen *et al.* 2008).

The *Lepus* remains from Oumm Qatafa and Tabun E (Garrad and Bate 1937), may be some of the earliest in the region as noted by Haas (1951) and Tchernov (1988), to which we can add more recent finds from Middle Pleistocene Hummal (Maul *et al.* 2015). Notably, *Lepus* appears simultaneously with *Ochotona* at Oumm Qatafa (see below). In subsequent Late Pleistocene assemblages, aside from the single occurrence of *Ochotona* in Qafzeh Cave, *Lepus* is the sole lagomorph represented (Tchernov 1988).

Family Ochotonidae

Genus *Ochotona*

Ochotona cf. rufescens Gray, 1842

Referred specimens: OQ-981 (D2), left hemimandible with m1; OQ-982 (D2), right hemimandible with p3-p4, and m2; OQ-983 (E1), left hemimandible with p4-m1; OQ-984 (E1), left hemimandible with p4-m1; OQ-985 (E1), left maxilla with two incisors I1-I2; OQ-986 (E1), mandibular fragment; OQ-987 (E1), left I1; OQ-988 (E2), right I1.

Taxonomic discussion: Vaufreij (1951) attributed two half mandibles from Layer D2 to *Lagomys* (the obsolete term for *Ochotona*). Another specimen was tentatively attributed to this species but was noted by him as deriving from Layer E3. Haas (1951) confirmed the specific identifications but listed two jaws

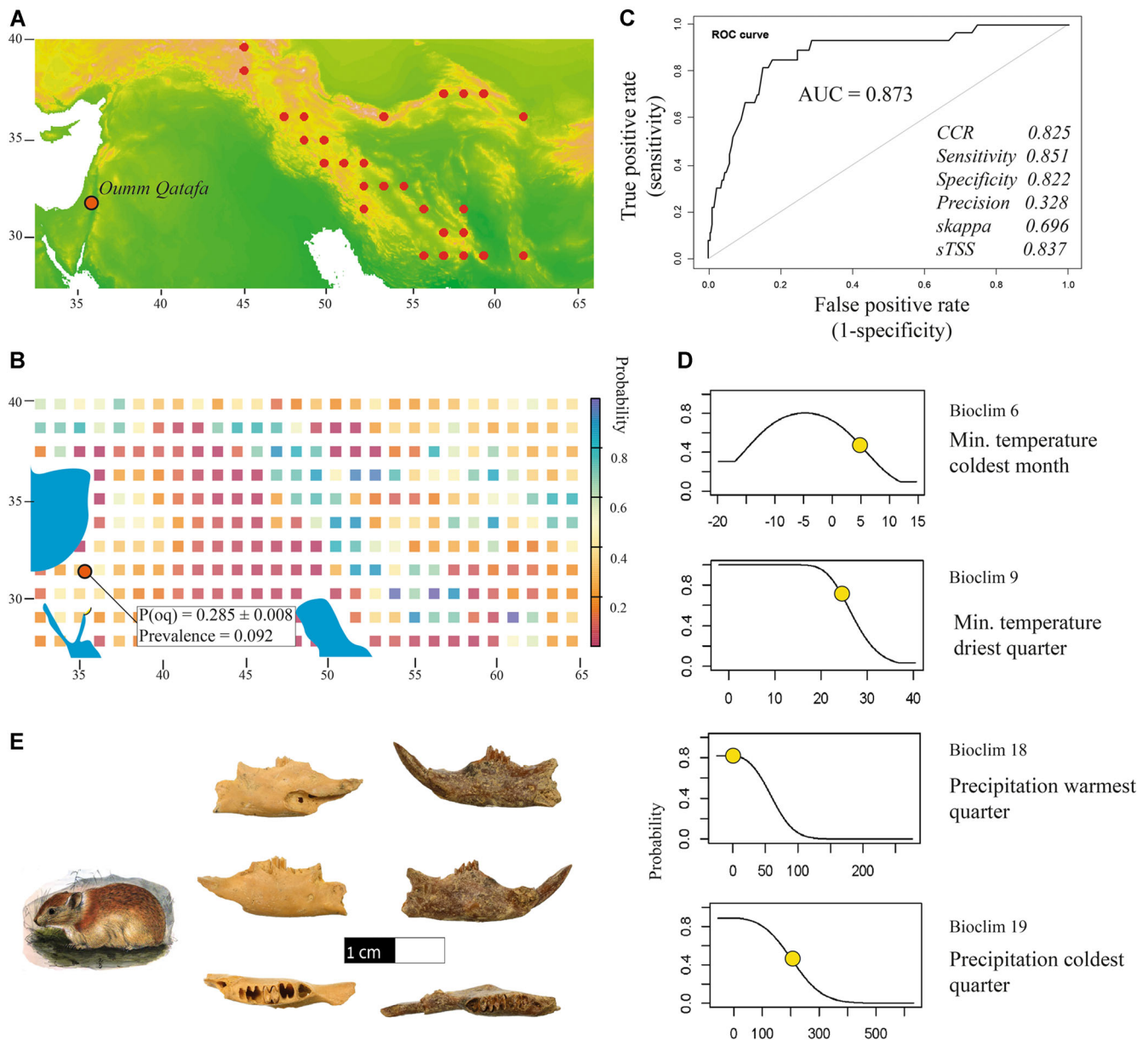


Figure 8. *Ochotona cf. rufescens*. (A) current occurrence data of *O. rufescens* and the location of Oumm Qatafa (basemap <https://chelsa-climate.org/>); (B) log probability values for finding suitable *O. rufescens* habitats based on the bioclimatic variables in the maxent model; $P(oq)$ is the probability for Oumm Qatafa today, confidence intervals obtained from modelling 1000 bootstrap samples of N-1 current observations; (C) area under the ROC curve ($AUC = 0.873$) and other model evaluation parameters obtained using the 'modEva' library (Barbosa *et al.* 2013) for binary predictions with a calculated optimal threshold 0.51 (not shown); (D) response curves for the four predictive bioclimatic variables, with the bioclimatic variable value at Oumm Qatafa today marked on each response curve; (E) specimens OQ-981 (left) and OQ-984 (right) in occlusal and buccal views; Afghan pika *O. rufescens* illustration by William Thomas Blanford (Blanford WT, 1876. *Eastern Persia: An Account of the Journeys of the Persian Boundary Commission 1871-72-73* by India Persian Boundary Commission). Downloaded from Wikipedia (https://en.wikipedia.org/wiki/Afghan_pika#/media/File:LagomysRufescens.jpg). Public domain. [Color figure can be viewed at [wileyonlinelibrary.com](https://onlinelibrary.com)]

from Layer E1 and two others from D2. Four lagomorph mandibles, two from Layer E1 and two from Layer D2, have been assigned following Haas (1951) and Tchernov (1988) to the genus *Ochotona*. They are too small to belong to *Lepus capensis*, and their dental morphology and tooth number follows that of pika (Fig. 8). The most common pika in the Middle East is *O. rufescens*, which is larger than the steppe pika *O. pusilla*. The measurements of two Oumm Qatafa mandibles, OQ-981 ($L_{p3-m3} = 11.05$ mm; $p3$ alveolus $L = 2.33$ mm, $B = 2.38$ mm) and OQ-984 ($L_{p3-m3} = 11.10$ mm; $p3$ alveolus $L = 2.01$ mm, $B = 2.35$ mm) straddle the upper range of recent specimens of the former taxon (Čermák *et al.* 2006) and should probably be assigned to *O. rufescens*.

Maxent modelling (Fig. 8; S13) suggests that habitat (as defined in a bioclimatic niche space) availability for *O. rufescens* is parsimoniously predicted by the minimum

temperature of the coldest month (bioclim 6), minimum temperature of the driest quarter (bioclim 9), precipitation in the warmest quarter (bioclim 18) and precipitation of the coldest quarter (bioclim 19). Plotting the prediction of the model on variable values alongside with the values at Oumm Qatafa today (Fig. 8D) suggests that the latter locale is currently marginal in view of the Afghan pika's climatic niche, with wetter and warmer winters than are optimal for the species. However, the model predicts 0.285 ± 0.008 probability of a suitable habitat around Oumm Qatafa today (based on $n = 1000$ bootstrap sampling of the current occurrence data), against a prevalence of 0.092. The analysis therefore suggests that the presence of Afghan pikas in Layers D or E does not indicate a drastically different climate to the one present in the region today.

Order Carnivora Bowdich, 1821

Family Hyaenidae Gray, 1821

Genus *Crocuta* Kaup, 1828.

Crocuta crocuta spelaea Goldfuss, 1823

Referred specimens: OQ-68 (D2), right p2; OQ-76 (E1), left p2; OQ-88 (?), right m1; OQ-89 (?), left P3.

Description: The most informative specimen is OQ-88, an isolated m1 in an advanced stage of wear but well preserved, which shows the typical characteristics of *Crocuta* lower carnassials, including an elongated trigonid ($L = 26.7$ mm) and a short talonid ($L = 3.8$ mm) (Fig. 9). The overall size of the m1 is especially telling as it is relatively wide ($B = 14.1$ mm) for its length ($L = 30$ mm) compared with extant *C. crocuta* and fits better within the range of size variation of Pleistocene *C. crocuta spelaea* (Fig. 10). The paraconid ($L = 16.1$ mm) is longer than the protoconid ($L = 11.1$ mm) and the metaconid is absent. OQ-89 is a small left maxillary fragment with a complete, slightly worn and well-preserved P3, parts of the alveoli of P2 and P4, and the ventral portion of the infraorbital foramen. The tooth is aligned with the P2 alveolus following the antero-posterior longitudinal axis of the dentary, which is the typical condition in *Crocuta*. In *Hyaena*, the P2 and P3 are

obliquely oriented with respect to this axis. The P3 in OQ-89 is small ($L = 20.8$ mm, $B = 15.7$ mm), relatively brachydont ($H = 21.7$ mm), and simple, with greatly reduced anterolingual and posterior tubercles. There is only ~21 mm from the ventral edge of the infraorbital foramen to the P3 gum line. Thus, OQ-89 likely belonged to a small individual. OQ-68 is a complete right p2 in early wear that is also rather small ($L = 20.8$ mm; $B = 15.7$ mm; $H = 21.7$ mm). OQ-76 is a fragmented second premolar.

Taxonomic discussion: Vaufrey described the finds of Hyaenidae in his 1931 paper. These finds include a P4, which he noted was small relative to a modern spotted hyena but attributable to this species; a very worn lower molar, characterised by its large size and reduced talonid, which he attributed to *Crocuta*. A proximal tibia that he assigned to striped hyena based on size has not been found in the collection. He also noted the presence of coprolites that are found in all layers except E3. In the 1951 paper he only listed *Hyaena crocuta* as present in Layers E1–2 and D2, and *Hyaena striata* in Layer D1 but with no description of which elements were represented.

In this revision, we assigned four craniodental remains to *C. crocuta spelaea*. The Oumm Qatafa m1 (OQ-88) is considerably



Figure 9. (A) *Vulpes vulpes* OQ-85 (?), right p3-p4; (B) *Crocuta crocuta spelaea* 1, 2 – OQ-89 (?), left P3; 3, 4 – OQ-88 (?), right m1 (right); (C) *Canis cf. mosbachensis* OQ-75 (E1), left dp4, from 1 – occlusal, 2 – buccal, 3 – lingual, 4 – posterior and 5 – anterior views. (Photographs by Roeie Shafir). [Color figure can be viewed at wileyonlinelibrary.com]

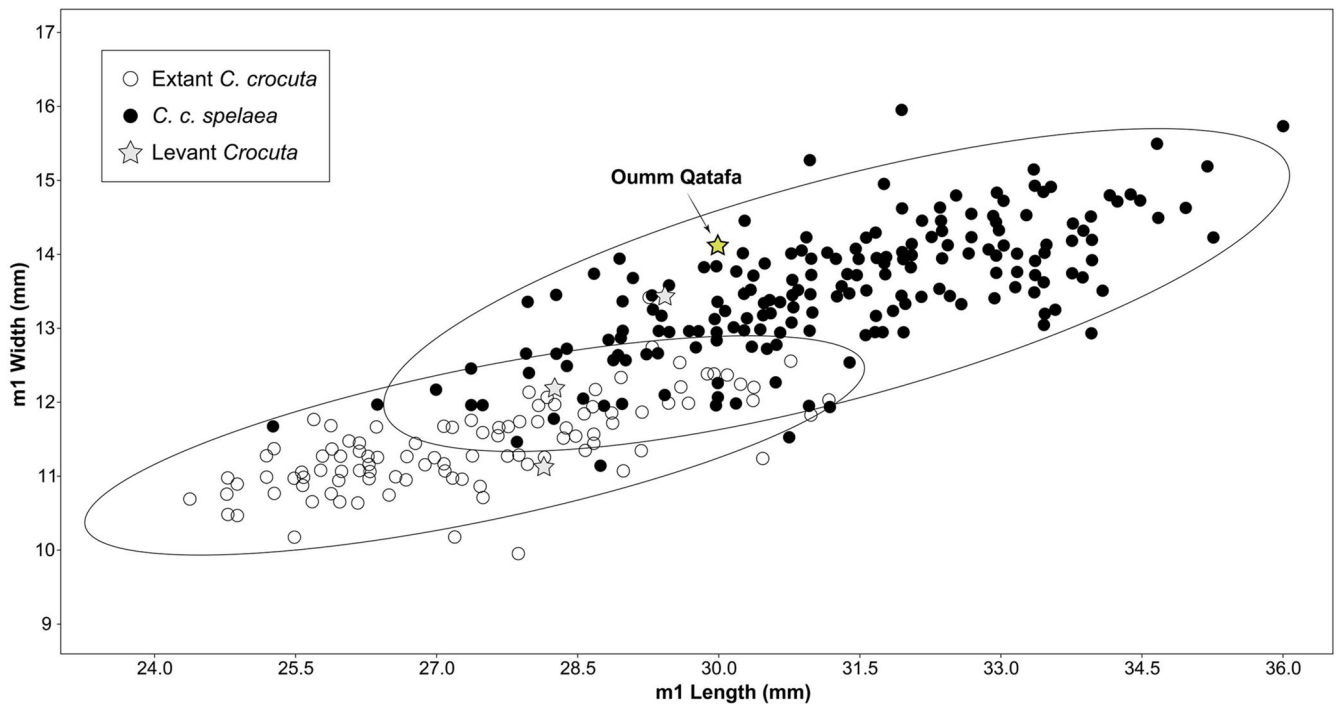


Figure 10. Dimensions of the lower carnassial in extant *Crocuta crocuta*, *C. crocuta spelaea* and selected *Crocuta* specimens from the Levant, including Oumm Qatafa. Data from Ballesio (1986), Hooijer (1961), Sauqué *et al.* (2017) and Tchernov and Tsoukala (1997). [Color figure can be viewed at [wileyonlinelibrary.com](https://onlinelibrary.wiley.com)]

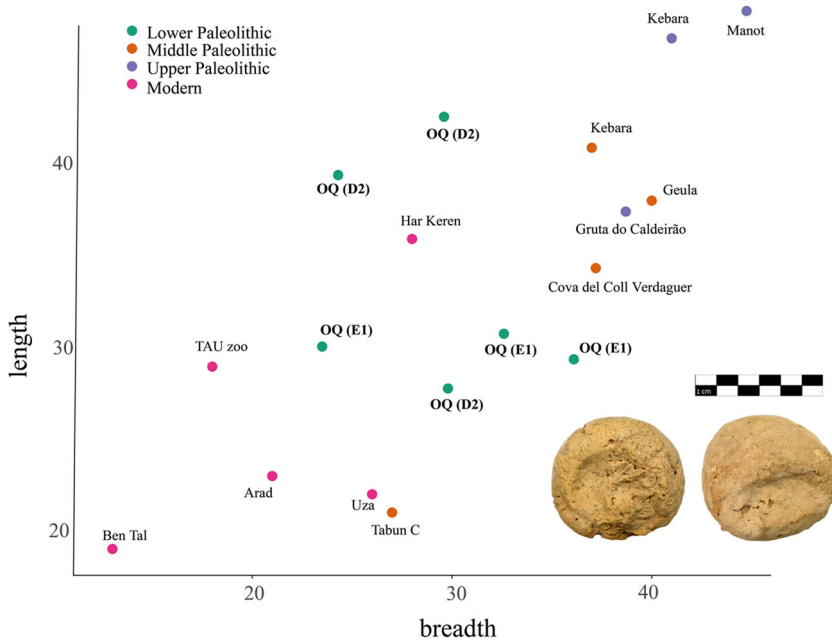


Figure 11. Maximal length and breadth of the hyaena coprolites from Oumm Qatafa (OQ) and published coprolites from recent and archaeological contexts (Davis *et al.* 2007; Horwitz and Goldberg 1989; Orbach and Yeshurun 2019). (Photograph of coprolite from Oumm Qatafa, Layer E1, by Roeef Shafir). [Color figure can be viewed at [wileyonlinelibrary.com](https://onlinelibrary.wiley.com)]

wider than in extant *C. crocuta* and fits better with other Pleistocene specimens of *C. crocuta spelaea* (Sauqué *et al.* 2017; Werdelin and Lewis 2008). The presence or absence of the metaconid in the lower carnassial is an extremely variable characteristic in extant and extinct spotted hyaenas, but the metaconid tends to be more developed in earlier *Crocuta* specimens than in later ones (Montes and Blasco 1997; Sauqué *et al.* 2017; Werdelin and Solounias 1991). The Oumm Qatafa premolars are rather small and simple but their size is compatible with smaller specimens of *C. crocuta spelaea*. In general, the hyaenid craniodental remains from Oumm Qatafa fit well with the typical small size of Pleistocene Levantine spotted hyaenas, which tend to be small (Fig. 10).

Six coprolites were found in the collection from Oumm Qatafa; three each from Layers E1 and D2. They show the characteristic form of hyaena coprolites, a rounded body with a dimple at the base and a short peak at the tip. They are comparable in shape to Late Pleistocene spotted hyaena coprolites from the Israeli sites of Kebara and Geula (Horwitz and Goldberg 1989) and Manot cave (Orbach and Yeshurun 2019; Table S5). When the maximal length and breadth of the coprolites from these sites are plotted, however, it appears that the Oumm Qatafa coprolites are small in relation to later coprolites from Late Pleistocene sites, although still on average larger than those of recent striped hyaenas (Fig. 11).

Family Canidae Fischer de Waldheim, 1817
Genus *Canis* Linnaeus, 1758

Canis cf. mosbachensis Soergel, 1925

Referred specimens: OQ-75 (E1), left dp4; OQ-82 (D2), isolated I2; OQ-99 (E1), right proximal radius; OQ-103 (?), left distal radius; OQ-104 (?), right proximal ulna; OQ-108 (E1), left p2; OQ-278 (E2), right dP4.

Taxonomic discussion: In his 1931 paper, Vaufrej described a fragment of a maxilla (from Layer E1) whose second and third molars were noted as broad, and the third molar was relatively large. He identified this specimen as belonging to *Canis aureus*, and suggested it belonged to the same animal (species) as a femur shaft from Layer D. Neither skeletal element has been found in the surviving faunal collection.

Seven post-cranial and craniodental fragments attributed to *Canis* were found in the assemblage. Some could be measured: OQ-103, a fused distal radius fragment (Bd = 19.9 mm; Dd = 29.2 mm), and OQ-104, a fused proximal ulnar fragment (DPA = 18.8 mm; SDO = 16.2 mm; BPC = ~12 mm), neither assigned to a layer. OQ-99, a fused proximal radius fragment (Bp = 14.4 mm; Dp = 9.8 mm) is assigned to Layer E1. OQ-278 is a dP4 with a large lingual basin with no cusps, unlike jackals and foxes. The specimen is quite small, but it matches the lower *Canis* dp4 (OQ-75) in size (MD = 6.0 mm; BL = 7.2 mm).

Of great interest is OQ-75, a complete left dp4, unerupted by its open root (Fig. 9). The specimen has a GL of 12.1 mm, and a talonid breadth (Wii) of 5.1 mm. A red fox can be excluded based on the size of OQ-75. Unfortunately, to the best of our knowledge, in-depth morphological studies of Pleistocene canid deciduous teeth do not exist; therefore, we resorted to a heuristic analysis based on geometric morphometrics. A comparative study of recent dp4 ($n = 31$) belonging to *Alopex*, *Lupullela*, *Urocyon*, *Nyctereutes*, *Lycaon*, *Canis* and *Vulpes* was undertaken (see SI2 for specimen details and analyses). Based on centroid size estimation (Fig. 12), specimen OQ-75 is beyond the range of canids other than *Lycaon pictus* and *Canis lupus*. Morphologically, *Lycaon* carnassials have a derived, hypercarnivorous blade-like morphology obtained through the loss of the hypoconid cusp of the talonid. Specimen OQ-75, however, has a hypotalonid; if morphologically the dp4 resembles the carnassials (Zack 2012), that would push our identification more in the direction of the genus *Canis*.

To further explore the specimen's shape, the transformed shape coordinates were subjected to shape principal component analysis (using the 'geomorph' package, Adams *et al.* 2021; see SI2). Specimen OQ-75 falls in the second quadrant of the resulting shape space, closely related to *Canis lupus* comparative specimens. The warp grids indicate a high trigonid-to-talonid width ratio, and a posteriorly compacted, albeit pointed, talonid shape. The first six principal components were then subjected to a canonical variate analysis (Fig. 12), meant to refine the identification of the specimen as *C. lupus* or an archaic *Lupullela*, e.g. *C. aureus* sensu lato. The result highlights the similarity of the OQ-75 shape to that of *C. lupus*.

Did the dp4 OQ-75 belong to a *C. lupus*, then? In our comparative sample, there exists a strong linear relationship between the talonid breadth (x) and GL (y) of canid dp4 ($y = 0.24 + 2.69x$; F-statistic: 383.3 on 1 and 30 DF, p -value: $< 2.2 \times 10^{-16}$, Adjusted $R^2 = 0.925$; Fig. 12C). The hypercarnivorous *Lycaon* premolars generally plot above the regression line: They are narrow and elongated. *Canis lupus* specimens generally plot on the regression line. OQ-75, however, falls far below the regression line, describing a broader tooth morphology. It shares the same size and proportions with a single other specimen – a dingo (*C. lupus dingo*), a feral and relatively omnivorous canid.

A comparison of centroid sizes therefore suggests that OQ-75 belongs in the smaller range of modern *Canis lupus* or *Lycaon pictus*; talonid morphology and occlusal outlines strongly suggest morphological similarity to the first, while rejecting identification as *Lupullela*. The length-to-width ratio of the tooth is relatively low, suggesting an omnivorous diet on a par with that of dingo, not wolf, within the genus *Canis*. These observations lead us to suggest that the specimen belonged to an archaic canid, although it is difficult to be more precise without proper diagnostic criteria for milk teeth. Based on the diagnostic criteria for m1 (Bartolini Lucenti and Rook 2016; Martínez-Navarro *et al.* 2009), the dp4 OQ-75 appears to be similar to the Arno River dog, *Canis arnensis* (Del Campana 1913): The paraconid has a straight, subvertical mesial margin; the protoconid is high and inclined distally; the metaconid is well-individualised from the protoconid and disto-lingually displaced; and the talonid basin is well developed with a larger hypoconid and a smaller entoconid. Two features are, however, missing: an accessory cuspid on the lingual edge of the talonid, and a low, strong hypoconulid shelf (Bartolini Lucenti and Rook 2016). We do not know whether these latter dissimilarities reflect a taxonomic difference between the Oumm Qatafa canid and *C. arnensis*, or whether they should be attributed to morphological variation between deciduous OQ-75 and the m1 of this extinct species. Given the Early Pleistocene chronostratigraphic association of *C. arnensis*, however, we here make the parsimonious assumption that the smaller, more omnivorous *Canis* species represented at Oumm Qatafa is the Mosbach Wolf, *Canis mosbachensis*, a species which first appeared in the region in the Early Pleistocene at 'Ubeidiya (Martínez-Navarro *et al.* 2009) and survived here throughout the Middle Pleistocene, as attested at sites such as the 'Bears Cave' (Tchernov and Tsoukala 1997).

Genus Vulpes (Gersault, 1764)

Vulpes vulpes (Linnaeus, 1758)

Referred specimens: OQ-85 (?), right p3-p4; OQ-86 (?), right distal radius; OQ-87 (?), radius diaphysis fragment; OQ-98 (D2), right distal radius fragment; OQ-108 (?), left p4; OQ-109 (E1), left dp4; OQ-110 (E1), right M1.

Taxonomic discussion: Seven specimens in the assemblage have been attributed to red fox, *Vulpes vulpes*, based on their size: OQ-85, right mandible with p3-p4 (p3 L = 8 mm, B = 2.6 mm; p4 L = 8.5 mm, B = 3.1 mm; premolar molar row length = 52.1 mm); OQ-86, right distal radius (AP = 7 mm; B = 12.9 mm); OQ-98, right distal radius (AP = 7.7 mm; B = 13.2 mm); OQ-108 is a p4 and OQ-110 is an unerupted M1 (L = 12.6 mm; GB = 6.4 mm; B = 4.6a), both from Layer E1. OQ-104 is a fused proximal ulna (SDO = 23.7 mm). Three species of fox currently inhabit the Judean Desert, *V. vulpes*, Blanford's fox (*Vulpes cana*) and Rüppel's fox (*Vulpes rueppellii*) but to date, neither of the latter two species have been identified in Middle Pleistocene or Late Pleistocene assemblages. The earliest *Vulpes* in the region, identified as cf. *V. praeglacialis*, is known from 'Ubeidiya (Martínez-Navarro *et al.* 2009), while aside from Oumm Qatafa, red fox is found in the roughly coeval Middle Pleistocene vertebrate assemblage from Give'at Shaul (Tchernov 1988) and possibly also in the Middle-Late Pleistocene fauna from Rantis Cave (Marder *et al.* 2011). In contrast to our revision, Vaufrej (1951) identified remains of fox only from the two uppermost layers of the site. In Layer D2 he identified two fragments of mandible and a small fragment of maxilla with molars which he initially termed as belonging to *Vulpes nilotica* (an alternate term for the red fox at that time) (Vaufrej 1931). In the 1951 publication they are correctly attributed by him to *V. vulpes*.

Family Felidae (Fischer von Waldheim, 1817)

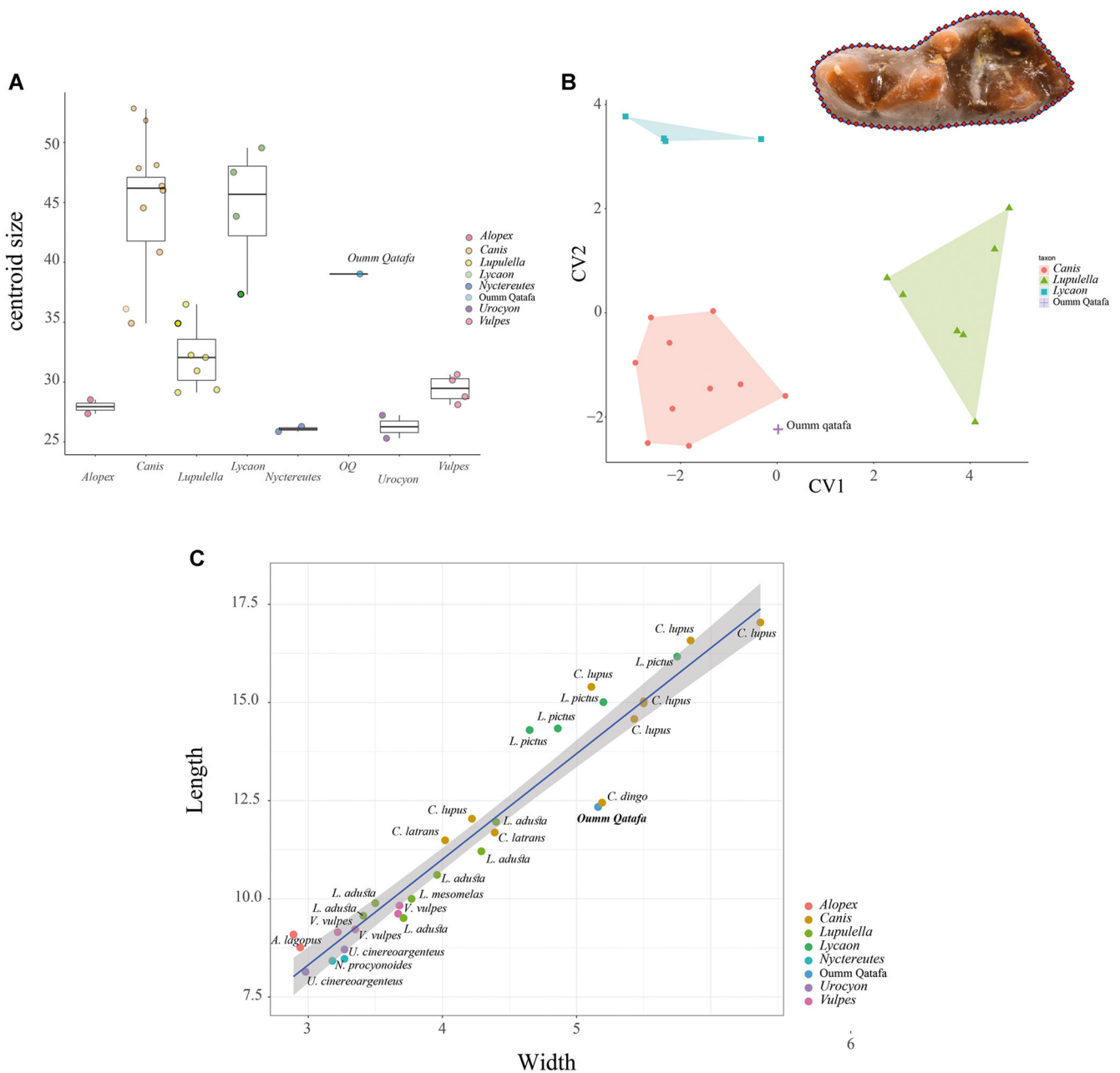


Figure 12. Size and shape of the *Canis* dp4 OQ-75. (A) centroid size compared with the dp4 of other canid taxa; (B) canonical variates analysis for the dp4 shape of Canid taxa. CV1 = 65.2%, CV2 = 31.7%; semi-landmark locations around tooth shown in inset; (C) the relationship between the maximum length and breadth of canid dp4s ($F = 421.9$, $DF = 30$, $p < 0.001$). Data and code in Supplement S2. [Color figure can be viewed at wileyonlinelibrary.com]

Genus *Felis* (Linnaeus, 1758)

Felis silvestris (Schreber, 1777)

Referred specimens: OQ-77 (E1), maxillary incisor; OQ-111 (?), proximal left ulna; OQ-112, left distal humerus.

Taxonomic discussion: Four specimens identified as wild cat, *Felis silvestris*, have been identified by us. Two of them yielded measurements that are in the range of modern *F. silvestris*: OQ-111 is a fused proximal ulnar fragment (DPA = 13.7 mm; SDO = 12.1 mm; BPC = 9.6 mm) and OQ-112 is an unfused humerus distal diaphysis fragment (SD = 5.9 mm), both from uncertain context.

In the 1931 paper, Vaufray noted the presence of a large wild cat (*Felis* cf. *silvestris*) represented by epiphyseal ends of a humerus, a proximal radius, a femur and distal tibia. In the 1951 paper, he listed that *Felis* cf. *silvestris* as represented by an ulna but lacked a layer attribution; and then other remains from layers E3 and D had no details as to skeletal elements

represented. Vaufray (1931) also listed a distal tibia from Layer D2 as belonging to a leopard *Felis pardus* (*Panthera pardus*) which has not been located by us. Remains of small felids are quite rare in Pleistocene sites from the Levant, and are often represented by isolated remains which limits their specific identification. A small felid, identified as 'the size of *F. silvestris*', is recorded at 'Ubeidiya (Martínez-Navarro *et al.* 2009), while aside from Oumm Qatafa, *F. silvestris* has been identified in Middle Pleistocene Revadim (Rabinovich *et al.* 2012).

Taphonomy

Retouchers: In Layers D1 and D2 Vaufray identified five bones that had been used as artefacts and retouched with flint tools. This includes two retouchers from Layer D2. d'Errico (1993) raised the possibility that one of these bones, a metatarsal, may

have served as a 'tensor' (a bone diaphysis furrowed with striae that are transverse to the bone's axis). Alternative functions have been suggested for tensors: implements used for stretching fibre for the fabrication of rope; musical instruments whereby a taut string is struck to produce sound; artefacts used to produce fire through friction of a fibre; and the most accepted function – implements used for retouching flint tools. None of these modified bones have been located by us and so could not be re-examined.

Burning: Neuville (1931, 1951) reports three burnt flints from the Tayacian II, Layers F to E3, and remarked (1931) that there were burnt bones in the Upper Acheulian levels at Oumm Qatafa, an observation that has been reiterated in the subsequent literature on the topic (e.g. Meignen *et al.* 2000; Rolland 2004: Table 3). Although no details are given in any of the publications as to the extent and nature of the Oumm Qatafa evidence, it is accepted as one of the few Levantine Late Acheulian examples for fire, joining the Upper Acheulian of Tabun level E (Garrod and Bate 1937; Jelinek *et al.* 1973; Shimelmitz *et al.* 2014), Acheulo-Yabrudian at Hayonim (Meignen *et al.* 2000) and Qesem Cave (Shahack-Gross *et al.* 2014).

In our analysis, we identified only 13 burnt bones in the Oumm Qatafa assemblage; three from Layer E and 10 from Layers D1–D2, although blackening by manganese staining was observed on 19–27% of the faunal specimens in the entire assemblage (Table 5). This degree of manganese staining can easily be confused with extensive burning, especially when the inner matrix of the bone is not exposed, revealing the superficial nature of the mineral staining (Shahack-Gross *et al.* 1997).

To further investigate the claim of burnt bones at the site, FTIR spectroscopic analysis was performed on 18 bones; one from Layer E2, one from Layer E1, one from Layer D, nine from Layer D2 and six with no layer attribution. Of these, 10 were

thought to be burnt based on visual observation on the state of discolouration (Table 6). The presence of burning in the FTIR plots was assessed based on the presence of a peak at 630 cm^{-1} attributed to hydroxylation of the bone mineral during exposure to heat above 600°C (Berna *et al.* 2012; Rey *et al.* 1995). We identified a prominent 630 cm^{-1} peak only in one specimen, the thoracic vertebra OQ-151 from Layer D2/38 (Fig. 13). Nine other faunal remains do not display a peak at all, and so are not burnt. All the other analysed faunal remains ($n=10$; Table 6) show the presence of a shoulder in the region of the 630 cm^{-1} peak but this we do not attribute to heat exposure (Fig. 14). Based on a series of spectroscopic experiments and data processing analysis (i.e. peak deconvolution), this shoulder cannot be attributed to vibrations corresponding to the OH groups and extrapolated to bone heated at lower temperatures. Instead, based on data analysis, this shoulder seems to be related to a new crystallographic phase of hydroxyapatite formed during burial at the bone surface through a process of dissolution and reprecipitation.

Breakage: The bone fragments from Layer D are larger on average (median length = 38 mm) than in Layer E (median length = 28 mm), which may be a result of compaction of the lower levels, especially due to the rockfall in Layer E2. There are more light-coloured bones (light-to-reddish ratio = 0.57) than in Layer E (ratio = 0.33) which probably reflects the sediment composition – a light brown clay in Layer D versus dark clay and silts in the lower levels.

Vaufrey (1931) noted that there were bones in all layers that exhibited anthropogenic fracturing. In this study we found that most specimens in both Layers E and D exhibited either dry or dry-on-green fracture morphologies, indicating diagenetic breakage of dry bone, often superimposed on bones originally fractured when fresh. Such fresh and dry breakage is illustrated in Vaufrey (1931: Fig. 31), along with what was interpreted by him as butchery and retouching marks. Since these specific bones are not in the curated collection and so could not be examined, it is difficult to say whether these modifications do not reflect trampling and carnivore damage, respectively.

Butchery and carnivore damage: Human butchery marks were observed only on five bones from Layers D1 and D2, although this might be an artefact of the larger sample size of this assemblage relative to the other layers. Despite their

Table 5. Taphonomic observations, see Methods for details.

Attribute	State	Layer E		Layers D1 & D2	
		N	%	N	%
length	mean	35.12		48.13	
	median	28		38	
	SD	31.39		30.55	
colour	light	7	25	16	36
	reddish	15	54	19	43
	brown	6	31	8	19
	black			1	2
staining	none	34	81	49	73
	few	3	7	5	7
	some	4	10	13	19
	many	1	2		
fractures	green, <50%			3	
	green, >50%				
	green, 100%				
	dry, <50%	1		2	
	dry, >50%				
	dry, 100%	1		2	
	mixed, <50%	1		3	
	mixed, >50%				
Abrasion		1		7	
		1		9	
Weathering			3		10
Burning				5	
Butchery	cut & percussion marks			1	
Gnawing				1	

Table 6. Fourier transform infrared spectroscopy results. Comparison of visual indications to burning with 630 cm^{-1} peak presence.

Specimen	Layer	Notes	Visual impression	630 cm^{-1} peak
OQ-1		tibia	burnt	no
OQ-2		tibia	burnt	no
OQ-19	D2	tooth	not burnt	maybe
OQ-46	D2	shaft	not burnt	no
OQ-48	D2	shaft	not burnt	no
OQ-49	D2	shaft	not burnt	maybe
OQ-51	D2	shaft	not burnt	no
OQ-56			burnt	no
OQ-62	E1	tibia	not burnt	maybe
OQ-130	E2	tooth	burnt	maybe
OQ-151	D2	vertebra	not burnt	yes
OQ-153	D2	mandible	not burnt	no
OQ-155	D2	vertebra	not burnt	maybe
OQ-173		shaft	burnt	no
OQ-187		mandible	burnt	no
OQ-196	D2	radius	burnt	maybe
OQ-207	D2	mandible	not burnt	maybe
OQ-225	D2	shaft	burnt	maybe
OQ-236		shaft	burnt	maybe
OQ-257	D2	tooth	burnt	maybe

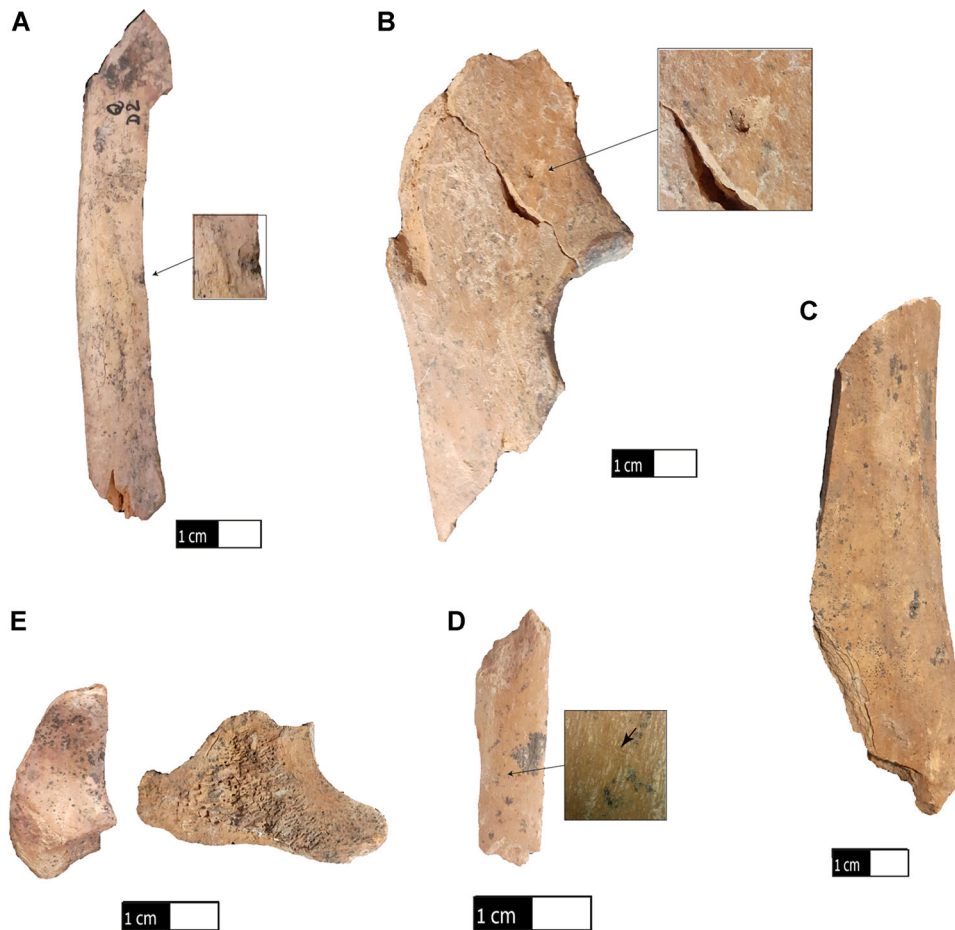


Figure 13. Taphonomically modified bones. (A–B) OQ-50, OQ-54, carnivore tooth punctures; (C) OQ-232, percussion flaking; (D) OQ-181, cut mark; (E) OQ-58, split phalanx. (Photographs by Liora K. Horwitz). [Color figure can be viewed at wileyonlinelibrary.com]

paucity, they provide solid evidence for an association between the fauna and human agency. A single specimen with a carnivore gnawing mark was also found in Layer D.

Discussion

The available faunal assemblage from Oumm Qatafa comprises 263 identified specimens. The number of specimens is unevenly represented for the different stratigraphic layers, which probably reflects their relative richness in each: 9 from Layer F, 64 from Layer E1, 62 from Layer D2 and 128 that are unassigned to a layer. A total of 15 genera are represented in the Oumm Qatafa assemblage, but the taxonomic diversity of the assemblages using combined counts for Layers D (D2 and D1; Late Acheulian) versus E (E3–1 Middle and Early Acheulean) show no significant difference across a range of indices (Tables 1 and 2). Moreover, the slight difference in the number of taxa between these units – 12 in Layer E and 14 in Layer D – is not significant following an individual rarefaction analysis (on PAST 4, Hammer *et al.* 2001: SI4).

Although the size of the overall assemblage that was studied is small, it shows a surprisingly rich species diversity. For example, there are five, possibly even six, different equid species in the assemblage: a large *E. ferus* form and *E. melkiensis*, whose fossils cannot be attributed to a layer; from Layer E2 a tentative identification of an equid related to the quagga, *E. aff. capensis*; two forms that both occur in Layers E and D2, *E. cf. mauritanicus* and *E. hydruntinus*; while *E. aff. africanus* appears to be constrained to the Late Acheulian Layer D. Thus, aside from a large caballine form (*E. ferus*), the

Oumm Qatafa assemblage contains two equid forms related to zebras (*E. mauritanicus* and a quagga *E. aff. capensis*), at least one form related to hemionies (*E. hydruntinus*), and two forms related to asses (*E. aff. africanus* and *E. melkiensis*). The diversity of equids emphasises the presence of suitable grassland environments in close proximity to the site in all phases.

Most of the macrofauna taxa identified from Oumm Qatafa can be found at contemporary sites in the Levant and can probably be assigned to the 'Qesem Faunal Unit' of the latest Middle Pleistocene (Belmaker 2009); some species, however, are more notable for their scarcity in Middle–Late Pleistocene sites. For example, the rhinoceros *Stephanorhinus hemitoechus*, which was a Pleistocene Palaearctic species widely distributed over parts of Europe, Asia and North Africa (Cerdeño 1998; Pandolfi and Tagliacozzo 2015; Pandolfi *et al.* 2020), is relatively rare in Southern Levantine Pleistocene sites, though it is likely the only rhino present from the Middle Pleistocene onwards. The remains from the Early Pleistocene site of 'Ubeidiya, dated to ~1.3 million years, have been attributed to *Stephanorhinus etruscus* (Guérin 1986; Pandolfi *et al.* 2017) while the records of *S. kirchbergensis* (formerly *Dicerorhinus mercki*) from Ksar' Akil in Lebanon and Tabun (Hooijer 1961) and Gesher Benot Ya'akov in Israel (Bar-Yosef and Tchernov 1972) are probably misidentifications and should be attributed to *S. hemitoechus* (Billia and Petronio 2009). Other Levantine sites with *S. hemitoechus* include Azraq Spring C, Abri Zumoffen, Masloukh and Tabun C–F, Skhul, Naamé, Tabun C–D, Dederiyeh Cave, Nadaouiyyeh Ain Askar, C-Spring, Ain Soda, and Shishan Marsh and likely also Gesher Benot Ya'akov and Geula (see references summarised

in Horwitz and Chazan 2007 and Pandolfi *et al.* 2020). The last appearance of rhino in the region, listed as an undetermined species, is documented in the Kebaran Layer C of Hayonim Cave (Davis 1982). *Stephanorhinus hemitoechus* likely inhabited steppe habitats for the most part, where it fed on grasses and forbs (Rivals and Lister 2016). There is direct evidence that this species was being consumed by Middle Pleistocene hominins thanks to the blood proteins matching Rhinocerotidae found in stone tools from Shishan Marsh 1 (Nowell *et al.* 2016).

Most of the large bovid remains from Oumm Qatafa are compatible with *Bos primigenius*. It is still unclear whether this species originated in Africa (Martínez-Navarro *et al.* 2012) or Asia (Gentry 2010), but its fossil record is most abundant in Eurasia and northern Africa and so can broadly be considered a Palaearctic element (see discussion in Aouraghe *et al.* 2021: 5–6). The earliest remains of *Bos* in the southern Levant are recorded from Early Pleistocene Daqara (Scardia *et al.* 2019) and the early Middle Pleistocene site of Geshar Benot Ya'akov, where it probably co-occurs with *Bison* (Martínez-Navarro and Rabinovich 2010). *Bos* occurs at later Middle Pleistocene sites in the Levant, including Abri Zumoffen, Masloukh, Tabun E/F, Revadim, Nahal Hesi, Qesem Cave and Holon (Stiner *et al.* 2009; Yeshurun *et al.* 2011; and summary in Horwitz and Chazan 2007: Table 13.2). The common Levantine herbivore taxa, *Gazella* and *Capra*, are represented throughout the sequence, probably by the forms *Gazella gazella* (mountain gazelle) and *Capra ibex*, in addition to two common species of cervids – *Cervus elaphus* (red deer) and *Dama mesopotamica* (fallow deer).

The carnivores of Oumm Qatafa are represented by *Crocota crocuta spelaea*, *Canis* cf. *mosbachensis*, *Vulpes vulpes*, and *Felis silvestris*. Early Acheulian sites that have yielded spotted hyaena remains include 'Ubeidiya and possibly Latamne and Evron Quarry (Tchernov 1988). Late Acheulian occurrences of Hyaenidae are recorded in the assemblages from Zuttiyeh (*Crocota*), Tabun Layer E (*Hyaena*) (Kurten 1965), Qesem Cave and Rantis – although the hyaenid species represented at the last two sites was not noted (Marder *et al.* 2011; Stiner *et al.* 2009). The latest occurrence of *Crocota* in the region was in the terminal Pleistocene of Kebara C (Kurten 1965; Bar-Oz and Weissbrod 2017), following which *Hyaena hyaena* became the sole representative of this family in the southern Levant (Lazagabaster *et al.* 2021a, 2022). Work in progress suggests that *Crocota* may have also been present in the southern Judean Desert during the latest Middle Pleistocene and in the latest Late Pleistocene. The hyaenid premolars from Oumm Qatafa are simple and small and the first molar is in the lower range of size variation of Eurasian *C. crocuta spelaea* and similar to that of other Pleistocene Levantine spotted hyaenas (Fig. 10). It is possible that the smaller size of the Pleistocene Levantine populations is related to the drier and hotter climate of the Levant in comparison with more septentrional regions, following to a certain extent Bergmann's rule. However, it is also possible that the Levantine population developed slightly different hunting/scavenging behaviour and may even represent a different subspecies. Interestingly, the six hyaenid coprolites from Oumm Qatafa are small in relation to later coprolites from Late Pleistocene sites, although still on average larger than those of recent striped hyaenas (Fig. 11). Thus, the size of the *Crocota* population from Oumm Qatafa seems to be relatively consistent and not an artefact of sample size.

A medium-sized *Canis* is also represented in the assemblage, notably by a deciduous premolar. In a late Middle Pleistocene setting, this *Canis* could potentially represent various species. The most common species identified in

Pleistocene assemblages are wolves (*Canis lupus* sbsp.) and jackals (Tchernov 1988), of which two different forms were thought to inhabit the Levantine Pleistocene cave assemblages (Bate 1937) – *C. aureus* (native to the Middle East) and *C. lupaster* (native to the Nilotic region of North Africa). Notably, Kurten (1965) only listed *C. lupaster* as present (in Zuttiyeh, Shukbah Level D, Tabun Levels D and E) based on the large size of the remains relative to those of the golden jackal. Additional canid taxa found in Early to Mid-Pleistocene sites are *Canis mosbachensis* identified at 'Ubeidiya (Tchernov 1988), and the African wild dog *Lycaon pictus* identified at Hayonim Layer E (Stiner *et al.* 2001). The *Canis* from Oumm Qatafa is too small to be a wolf, too large and morphologically different from a jackal, and too late chronologically to be the smaller, jackal-like canid which it resembles most morphologically, *Canis arnensis*. In terms of chronology, it would best suit *Canis mosbachensis*. As we do not have enough information to confirm whether the m1 morphological differences hold for the dp4, we are left with the most viable option, which is *C. mosbachensis*, and assume for now that the dp4s are not diagnostic until further work shows otherwise. We conclude that the Oumm Qatafa specimen represents a smaller and more omnivorous member of the genus *Canis* than *Canis lupus* and assume it to have been *Canis mosbachensis* on chronostratigraphic grounds.

Two genera of lagomorphs are found at Oumm Qatafa – *Lepus* and *Ochotona* – emphasising the diversity of this small assemblage. The genus *Ochotona* is known from west Asia since the Pliocene (cf. Sen *et al.* 2017) and *Ochotona* cf. *rufescens*, the Afghan pika or a species very similar to it, is known from Middle Pleistocene central Asia (Erbaeva 1988, reported in Čermák *et al.* 2006). In the southern Levant its unique occurrence in Oumm Qatafa is associated with a Middle Pleistocene inflow Palaearctic and Asian fauna (Tchernov 1992) and is not known from other locales. It is today the common pika in the Middle East, therefore giving us a rare chance to discuss palaeoenvironments based on the distribution of an extant species. The high frequency of hyrax is not unexpected given the rugged topography and current phytogeographic location of Oumm Qatafa. However, remains of hyrax are uncommon in Middle Pleistocene assemblages in the Levant, making Oumm Qatafa, Tabun Layers E–G (Garrod and Bate 1937) and Qesem Cave (Maul *et al.* 2016) the earliest occurrences of this species in the region apart from the early Mid-Pleistocene site of Geshar Benot Ya'akov (Goren-Inbar *et al.* 2000). Their remains do occur in several later assemblages, such as in Tabun D and Rantis Cave (Marder *et al.* 2011).

Although the size of the assemblage appears to be small, Oumm Qatafa is an important addition in view of the paucity of later Middle Pleistocene faunal assemblages from the region. This collection also establishes the presence of new species which are absent from contemporary sites – an equid (*Equus melkiensis*), canid (*Canis* cf. *mosbachensis*) and a lagomorph (*Ochotona* cf. *rufescens*) – and so enriches the biodiversity of this period as known to us. Oumm Qatafa is doubly important because it is the only faunal assemblage of that period from what is today a biogeographical boundary zone defining the eastern margin of the Levantine corridor out of Africa, which has been used since the Early Pleistocene as a major route by hominin expansions from Africa to Eurasia. In this work, the unique location in a biogeographical corridor and in an ecotonal zone between steppe and Mediterranean environments is evident in the transient presence of *Equus melkiensis* with an Asian first appearance datum and African last appearance datum, together with early occurrences of ochotonids, canids, and equids of Palaearctic origins.

In relation to Vaufrey's work, our study has added data on the relative frequency of taxa at the site. In all layers and for the assemblage, medium-sized to small herbivores predominate, with a clear dominance of goats (*Capra cf. ibex*) and hyrax. Large herbivores (equids, aurochs and rhino) are far less common, while the carnivore-to-herbivore ratios are also low; 12.5% for Layer E, 4.8% for Layer D and 8% for the assemblage as a whole. We have also clarified the specific identifications of the rhino (to the steppe rhino) and the gazelle (to mountain gazelle) and suggested the presence of a canid taxon new to the region. On the other hand, in some respects our taxonomic list is impoverished relative to the original (or at least not confirmed), due to the loss of some specimens. For example, Vaufrey (1951) identified a lower molar (without a layer attribution) as belonging to *Bubalis boselaphus* (currently *Alcelaphus bucelaphus*). This piece has not been located by us. *Alcelaphus* is rare in Middle Pleistocene assemblages from the Levant and has only been documented in Tabun Layers E/F (Tchernov 1988). Likewise, a first metacarpal from a bear (*Ursus arctos syriacus*) that was noted by Vaufrey (1931, 1951) as present in Layer D1 has not been relocated by us, neither have the *Canis aureus* maxilla (Layer E1) and femur (Layer D) he identified. In contrast, we have augmented the number of equid taxa identified.

Our analysis has also contributed a taphonomic description of Layers E (combined 1 to 3) and D (combined D1 and 2). The skeletal elements represented in the assemblage (Table 3) are quite evenly distributed between layers with far more cranial elements, especially mandibles and maxilla, over post-cranials in both the Layer E complex (83%) and Layer D complex (66%) and in the assemblage as a whole (72%). Undoubtedly, the selective retention of these elements over post-cranials for palaeontological analysis by Neuville has biased the assemblage, limiting application of accepted taphonomic criteria for determination of the agents responsible for the faunal assemblages (e.g. Lyman 1995, Kuhn *et al.* 2010, Fernández and Andrews 2016). The fauna from the earlier stratum, Layer E, have a darker colouration, higher percentage of manganese staining, smaller mean fragment size, and higher frequency of 'dry' fractures. The later assemblage shows more abrasion and weathering. These taphonomic observations suggest dissimilarity in the diagenetic trajectory typical of the earlier and later layers (E complex versus D) in Oumm Qatafa and is associated in part with variation in the sedimentary contexts (soil type), higher water activity (associated with abrasion and manganese staining) as well as heavier overburden leading to compaction of fauna in the earlier, lower levels than those above.

In both contexts, however, evidence for carnivore involvement in the assemblage formation is scarce despite the presence of skeletal remains of three different taxa: spotted hyaena, two canid species and a small felid. Human modifications are more common in the larger Late Acheulian Layer D assemblage and include both burning and cut marks. Importantly, although only one bone proved to be burnt based on FTIR analysis, this method cannot identify bones burnt at temperatures lower than 600°C. Thus, some if not all of the bones we suspect were burnt may still have been exposed indirectly to fire. In the same context, carnivore gnawing has been observed only on a single specimen. Humans are therefore favoured as the major bone-accumulating agent, at least in Layer D. However, the paucity of anthropogenic or carnivore damage in Layer E makes it more difficult to assess which agents were responsible for this assemblage. There are, however, some species-specific indicators; features that are not observed on remains of all species. For example, the consistent damage pattern observed on the partial tooth rows for hyrax resembles that observed in hyaena dens (missing

ramus, destruction of the underside of the mandibular corpus and the anterior portion of the jaw, e.g. Horwitz and Smith 1988). It raises the possibility that a carnivore, probably a hyaena, may in fact be the agent responsible for introducing most of the hyrax remains into the cave.

Global prehistory has been governed by the effects of climate change (e.g. Behrensmeier 2006; Breeze *et al.* 2016; Marean *et al.* 2015; deMenocal 2011). Its specific impact on past faunal and floral biodiversity is a matter of current concern since present-day biodiversity, which reflects ecosystem resilience (Willis *et al.* 2010), has been moulded by historical events. Climate change responses in organisms can lead to a loss of species richness following fragmentation or loss of habitats, or a change in species range or physiology acting through shifts in resource availability (Bellard *et al.* 2012). If the rate and magnitude of climate change is severe, it can also result in restriction of species range, species extirpation and even extinction. Tracking climate change in the past is challenging – especially at different biome levels (the local, regional and ecosystem) – due to problems of chronological control, variability in faunal assemblage size, differences in responses of ecologically different species to climatic changes and the wide spectrum of biotic and abiotic factors that may have influenced the composition of palaeofaunal assemblages, not least being anthropogenic impacts (Faith and Lyman 2019). Despite these problems, the extent and pace of such change becomes apparent when interpreting long-term palaeoecological data sets, especially those from a constrained geographical region (e.g. Davis 1982; Lyman 2016).

Here, the unique biogeographical position of the site of Oumm Qatafa at the boundary between today's Mediterranean and desert zones assumes special importance. The new quantification of the taxonomic composition undertaken here enables the comparison of the Oumm Qatafa fauna with other sites and so has enlarged the late Middle Pleistocene mammalian communities known to us. The comparison with other Levantine sites of similar Middle Pleistocene chronology (for the raw data, see Horwitz and Chazan 2007) can be summarised by a correspondence analysis biplot (Fig. 15, data in Supplement S14), which appears to separate the sites into coastal wetlands (the open-air sites of Holon and Revadim Quarry), in which mega-herbivores such as hippopotamus and straight-tusked elephant can be found; Mediterranean forest (the caves of Abri Zumoffen, Qesem, Tabun E/F, Masloukh), in which wild boar and deer dominate; and a steppe/desert (Azraq Spring C) which is set apart from the rest by a dominance of large grazers: camelids, and to a lesser extent rhinos and horses. Oumm Qatafa's distinctive location at a hitherto unexplored boundary zone is made obvious in the biplot, with arid- and cliff-adapted caprines (ibex) distinguishing Oumm Qatafa from most sites in the Mediterranean zone. The fact that this intersite comparison shows patterns that can be explained by current environmental and phytogeographical gradients suggests, in and by itself, the lasting stability of these environmental divisions in the longue durée. The arid conditions typical of the Oumm Qatafa boundary zone suggest open landscapes of Irano-Turanian character in which the steppe rhino, cursorial canids and hyaenids and several different species of equids could exist, along with ibex and pika where the topographical relief was sharper. As we have shown, Oumm Qatafa today has a climate that is probably within the climatic tolerance limits of extant pikas, albeit too warm and wet. Pikas, however, are very resilient to climate change (Smith 2020).

Given that, the presence of cervids does suggest a somewhat thicker vegetation cover, probably to the west of the site.

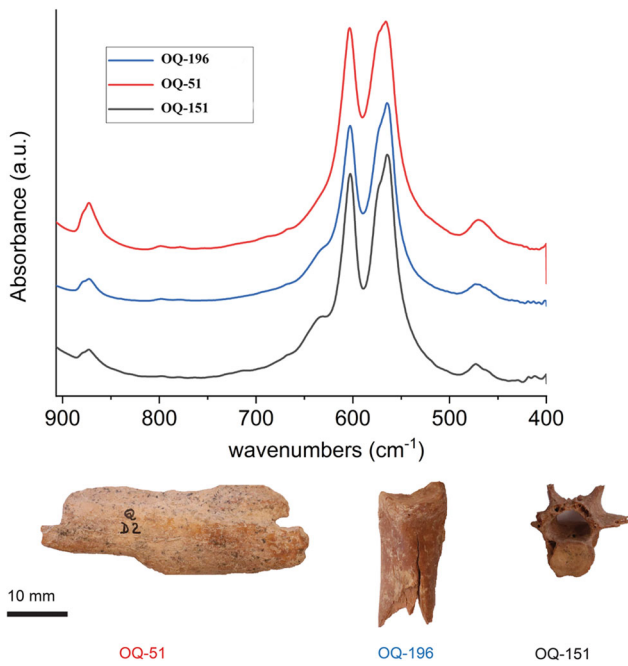


Figure 14. Fourier transform infrared spectroscopy spectra for representative specimens with different shapes of the 630 cm⁻¹. [Color figure can be viewed at wileyonlinelibrary.com]

Similarly, the identification of the Palestine Mountain Gazelle, *Gazella gazella* rather than its arid-adapted vicariant *Gazella dorcas*, suggests somewhat more mesic conditions. The body size of hyrax, which is sensitive to climatic change, appears to covary with the size range of sub-Saharan conspecifics than with the regionally extant Arabian subspecies. This, again, suggests a moister climate. And finally, in 1991 when teeth were removed from a layer attributed to D2 for ESR dating (Porat *et al.* 1992, 2002), a sediment sample was also taken from a clay layer below the teeth for pollen analysis. The sample (with a pollen count of 63; Supplement S15) indicated a Mediterranean regime that included oaks and conifers as well as some steppe forms. Horowitz (1992: 413) assigned this sample to the middle part of his palynozone QVII which was characterised by a pluvial climate (Horowitz 1989).

Conclusion

The Oumm Qatafa faunal assemblage reflects climatic conditions somewhat more mesic than the current ones. All in all, the available data suggest that in the late Middle Pleistocene, the site was located, as it is today, in an ecotone between (probably open) forest and steppe. The diversity of large grazers and large carnivores and the large body size of hyrax and gazelle, indicate a higher carrying capacity in the steppe

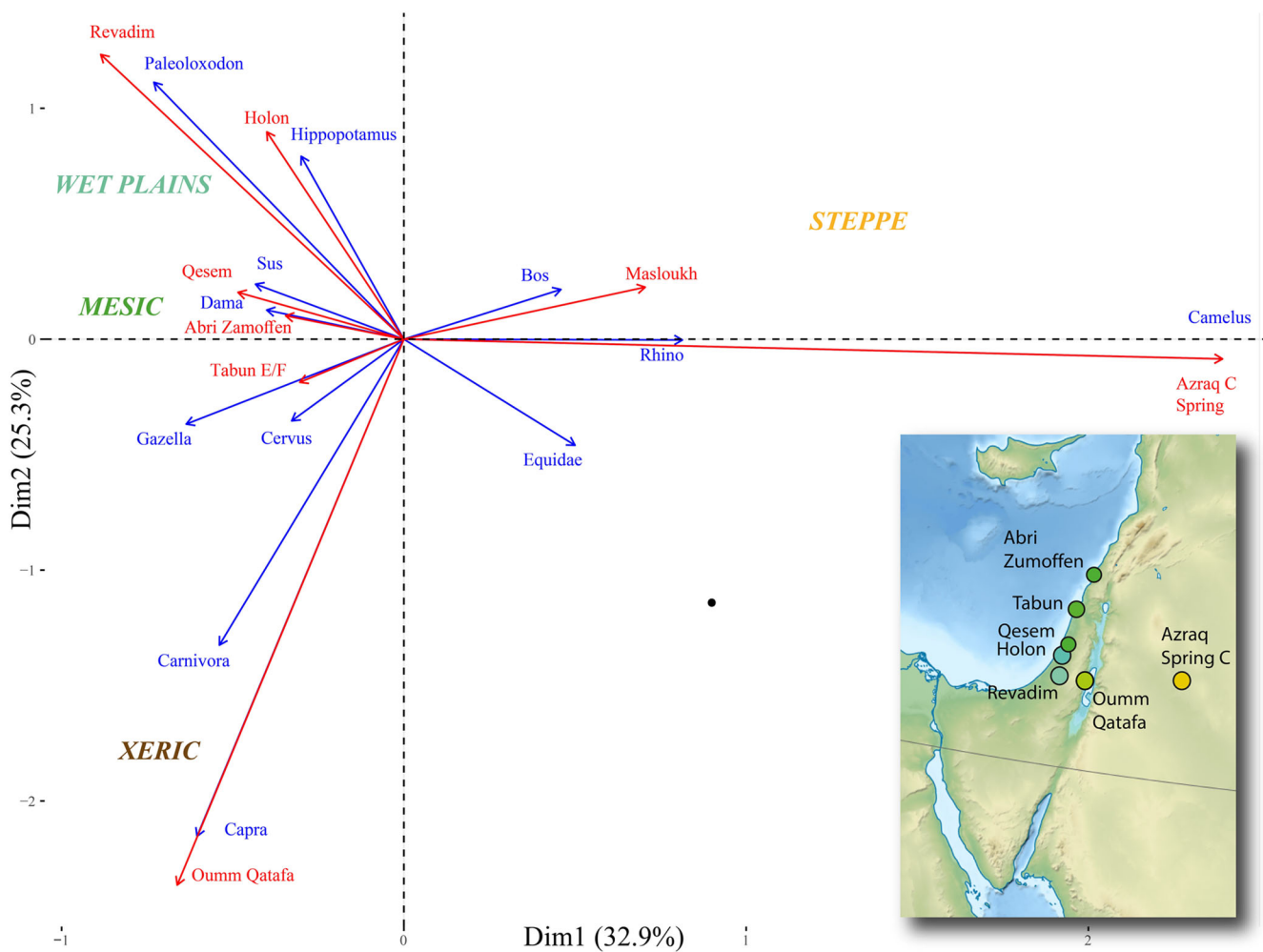


Figure 15. Correspondence analysis biplot for late Middle Pleistocene faunal assemblages in the Levant. Arrow length indicates effect size. Data in Supplement S4. [Color figure can be viewed at wileyonlinelibrary.com]

region, as do the deer for the forest environment. The boundary zone, while maintaining the current west-to-east cline in aridity, fell between grassland and forest, as opposed to remnant (and slightly distant) xeric Mediterranean woodland and hyperarid desert, as today. The extant species represented occur today in suitable but marginal habitats that currently exist within a 10–20 km radius of the site.

Oumm Qatafa is of great value because it is the only late Middle Pleistocene faunal assemblage known from the biogeographical boundary zone that today defines the eastern margin of the Levantine corridor, a route that has been used since the Early Pleistocene as a major conduit for hominin expansions from Africa into Eurasia (e.g. Bar-Yosef and Belfer-Cohen 2001; Goren-Inbar and Speth 2004; Wurz and Van Peer 2012). Moreover, for the estimated time period covered by this site (~500–200 kya; i.e. MIS 12 to 7), palaeoclimatic data for the region are fragmentary, i.e. speleothem records do not go beyond 250 ka (e.g. Bar-Matthews *et al.* 2017), making it doubly important. Unfortunately, the chronology of Middle Pleistocene sites with fauna (summaries in Horwitz and Chazan 2007) as well as pollen cores that span this time period (Horowitz 1989, 1992), is not very refined or complete. Thus, although the available data overall support the reconstruction of more mesic conditions in the region during interglacials, while during glacial periods forests tended to be replaced by open vegetation, it is not possible to track these climate shifts in the archaeological record. This is applicable as well to the Oumm Qatafa faunal assemblages, which are of very small size per layer, suffer from an inherent sampling bias and lack a robust chronology. We are only able to conclude from this record that slightly moister conditions than at present prevailed in the late Middle Pleistocene of the southern Levant.

Acknowledgements. Special thanks to Myriam Boudadi-Maligne for information relating to the *Canis* identification; to Aya Marck for her help in drawing Fig. 2; to Meir Orbach for fruitful discussion on hyaenas and canids; to Aharon Horowitz for permission to publish his pollen data from Oumm Qatafa; and to Shiri Ellenbogen of the CT unit in Tel Aviv University. We also wish to thank two anonymous reviewers. This research was supported by the European Research Council (Grant #802752, DEADSEA_ECO). IAL acknowledges the Humboldt Foundation and the University of Haifa for supporting his postdoctoral work.

Supporting information

Additional supporting information can be found in the online version of this article. This article includes online-only Supplemental Data.

- 1) SI1: Bone measurements in mm. Abbreviations follow von den Driesch (1976). Vera Eisenmann's measurements of equid bones are presented by element in separate Excel sheets.
- 2) SI2: R code and supplementary files for the morphometric analysis of OQ-75. "OQ_dp4.nb.html" presents the code and output.
- 3) SI3: R code and supplementary files for the maxent distribution modelling of *O. rufescens*.
- 4) SI4: Comparison of diversity indices between Layers D and E.
- 5) SI5: Aharon Horowitz's preliminary report on the pollen sampled in 1991 from Layer D2.
- 6) Supplementary figures:

Figure A. *E. aff. capensis*. OQ 122 (E2), left Tibia, A: anterior view, B: distal view; OQ 124 (E2), left Talus, C: posterior view, D: anterior view, E: distal view, F: medial view; G: OQ 123

(E2), left Calcaneum medial view. H: OQ 125 (?), first anterior Phalanx, profile. (Photographs by Roe Shafir and Vera Eisenmann).

Figure B. *E. aff. capensis* (A to I); *Equus hydruntinus* (J).

OQ 113 (E1) lower right dP4, A and B: occlusal view and scan; OQ 114 (E1) upper right dP4, C and D: occlusal view and scan; OQ 115 (E1) upper left dP4, E, F and G: occlusal view and scans; OQ 118 (F 32/23), H and I: section and vetibular view of a lower left molar germ. *Equus hydruntinus*, OQ 116 (E2/3), upper left dl3, J: occlusal view. (Photographs by Roe Shafir).

Figure C. Simpson's diagrams of *E. (Asinus) aff. africanus* from Ain Metherchem, Tunisia and *E. (Quagga) mauritanicus* from Tighenif, Algeria MC. 1: maximal length. 3: breadth at the middle of the diaphysis. 4: depth of the diaphysis at the same level. 5: proximal breadth. 6: proximal depth. 10: distal supra-articular breadth. 11: distal articular breadth. 12: depth of the sagittal crest. 13: least depth of the medial condyle. 14: greatest depth of the medial condyle. *n*: number of specimens.

References

- Adams DC, Collyer ML, Kaliontzopoulou A *et al.* 2021. *Geomorph: Software for geometric morphometric analyses* (Version R package version 3.3.2) [Windows]. <https://cran.r-project.org/package=geomorph>
- Aouadi N, Dridi Y, Ben, Dhia W. 2014. Holocene environment and subsistence patterns from Capsian and Neolithic sites in Tunisia. *Quaternary International* **320**: 3–14.
- Aouraghe H, van der Made J, Haddoumi H *et al.* 2021. New materials of the white rhinoceros *Ceratotherium simum* and aurochs *Bos primigenius* from a Late Pleistocene terrace of the Oued el Haï (NE Morocco)-two elements of the Maghrebi Palearctic fauna. *Historical Biology*. <https://doi.org/10.1080/08912963.2021.1995381>
- Asperen EN, Kahlke RD. 2015. Dietary variation and overlap in Central and Northwest European *Stephanorhinus kirchbergensis* and *S. hemitoechus* (Rhinocerotidae, Mammalia) influenced by habitat diversity: "You'll have to take pot luck!" (proverb). *Quaternary Science Reviews* **107**: 47–61.
- Bagtache B, Hadjouis D, Eisenmann V. 1984. Présence d'un *Equus* caballin (*E. algericus* n. sp.) et d'une autre espèce nouvelle d'*Equus* (*E. melkiensis* n. sp.) dans l'Atérien des Allobroges. *Algérie. Comptes-Rendus Des Séances de l'Académie Des Sciences* **298**(14): 609–612.
- Ballesio R. 1986. Les Carnivores du gisement Pléistocène d'Oubéidiyeh. In *Les Mammifères du Pléistocène Inférieur, de la Vallée du Jourdain à Oubéidiyeh*, Tchernov E (ed). Assoc. Paléorient: Paris; 63–92.
- Barbosa AM, Real R, Munoz AR *et al.* 2013. New measures for assessing model equilibrium and prediction mismatch in species distribution models. *Diversity and Distributions* **19**(10): 1333–1338.
- Bar-Matthews M, Ayalon A, Vaks A *et al.* 2017. Climate and environment reconstructions based on speleothems from the Levant. In *Quaternary of the Levant*, Enzel Y, Bar-Yosef O (eds). Cambridge University Press: Cambridge; 151–164.
- Bar-Oz G, Weissbrod L. 2017. The kaleidoscope of mammalian faunas during the Terminal Pleistocene and Holocene in the Southern Levant. In *Quaternary of the Levant*, Enzel Y, Bar-Yosef O (eds). Cambridge University Press: Cambridge 363–368.
- Bartolini Lucenti S, Rook L. 2016. A review on the Late Villafranchian medium-sized canid *Canis arvensis* based on the evidence from Poggio Rosso (Tuscany, Italy). *Quaternary Science Reviews* **151**: 58–71.
- Bar-Yosef O. 1994. The Lower Paleolithic of the Near East. *Journal of World Prehistory* **8**(3): 211–265.
- Bar-Yosef O, Belfer-Cohen A. 2001. From Africa to Eurasia - early dispersals. *Quaternary International* **75**(1): 19–28.
- Bar-Yosef O, Belmaker M. 2011. Early and Middle Pleistocene faunal and hominins dispersals through Southwestern Asia. *Quaternary Science Reviews* **30**(11–12): 1318–1337.

- Bar-Yosef O, Chernov E. 1972. *On the Palaeo-Ecological History of the Site of Ubeidiya*. Israel Academy of Human Sciences and Humanities: Jerusalem.
- Bate DAM. 1937. *Palaeontology: The Fossil Fauna of the Wady El-Mughara Caves: Vol. II*. Clarendon Press.
- Behrensmeyer AK. 2006. Climate change and human evolution. *Science* **311**(5760): 476–478.
- Belmaker M. 2009. Hominin Adaptability and Patterns of Faunal Turnover in the Early to Middle Pleistocene Transition in the Levant. In *Sourcebook of Paleolithic Transitions*, Camps M, Chauhan P (eds). Springer, 211–227.
- Bellard C, Bertelsmeier C, Leadley P *et al.* 2012. Impacts of climate change on the future of biodiversity. *Ecology Letters* **15**(4): 365–377.
- Ben Slimen H, Suchentrunk F, Stamatis C *et al.* 2008. Population genetics of Cape and brown hares (*Lepus capensis* and *L. europaeus*): A test of Petter's hypothesis of conspecificity. *Biochemical Systematics and Ecology* **36**: 22–39.
- Berna F, Goldberg P, Horwitz LK *et al.* 2012. Microstratigraphic evidence of in situ fire in the Acheulean strata of Wonderwerk Cave, Northern Cape province, South Africa. *Proceedings of the National Academy of Sciences* **109**(20): E1215–E1220.
- Bernor RL, Cirilli O, Jukar AM *et al.* 2019. Evolution of Early *Equus* in Italy, Georgia, the Indian Subcontinent, East Africa, and the Origins of African Zebras. *Frontiers in Ecology and Evolution* **7**. <https://doi.org/10.3389/fevo.2019.00166>
- Billia EM, Petronio C. 2009. Selected records of *Stephanorhinus kirchbergensis* (Jäger, 1839) (Mammalia, Rhinocerotidae) in Italy. *Bollettino della Società Paleontologica Italiana* **48**(1): 21–32.
- Boessneck J, Müller H-H, Teichert M. 1964. Osteologische Unterscheidungsmerkmale zwischen Schaf (*Ovis aries* Linné) und Ziege (*Capra hircus* Linné). *Kühn-Archiv* **78**: 1–129.
- Brain CK. 1983. *The Hunters Or the Hunted?: An Introduction to African Cave Taphonomy*. University of Chicago Press: Chicago.
- Breeze PS, Groucutt HS, Drake NA *et al.* 2016. Palaeohydrological corridors for hominin dispersals in the Middle East 250–70,000 years ago. *Quaternary Science Reviews* **144**: 155–185.
- Cerdeño E. 1998. Diversity and evolutionary trends of the Family Rhinocerotidae (Perissodactyla). *Palaeogeography, Palaeoclimatology, Palaeoecology* **141**(1–2): 13–34.
- Čermák S, Obuch S, Benda P. 2006. Notes on the genus *Ochotona* in the Middle East (Lagomorpha: Ochotonidae). *Lynx (Praha)* **37**: 51–66.
- Danin A. 1988. Flora and vegetation of Israel and adjacent regions. In *The Zoogeography of Israel*, Yom-Tov Y, Tchernov E (eds) Dr. W. Junk Publishers: Dordrecht; 129–158.
- Davis S. 1977. The ungulate remains from Kebara Cave. *Eretz Israel* **13**: 150–163.
- Davis SJM. 1980a. Late Pleistocene and Holocene equid remains from Israel. *Zoological Journal of the Linnean Society* **70**(3): 289–312.
- Davis SJM. 1980b. Late Pleistocene Holocene gazelles of northern Israel. *Israel Journal of Ecology and Evolution* **29**: 135–140.
- Davis SJM. 1982. Climatic change and the advent of domestication: the succession of ruminant artiodactyls in the Late Pleistocene-Holocene in the Israel region. *Paléorient* **8**(2): 5–15.
- Davis SJM, Robert I, Zilhão J. 2007. Caldeirão cave (Central Portugal)- whose home? Hyaena, man, bearded vulture. *Courier-Forschungsinstitut Senckenberg* **259**: 213.
- deMenocal PB. 2011. Anthropology, climate and human evolution. *Science* **331**(6017): 540–542.
- Demirbaş Y, Albayrak I. 2014. The taxonomic status and geographic distribution of the European hare (*Lepus europaeus* Pallas, 1778) in Turkey (Mammalia: Lagomorpha). *Turkish Journal of Zoology* **38**: 119–130.
- D'Errico F. 1993. Criteria for identifying utilised bone: the case of the Cantabrian "tensors". *Current Anthropology* **34**(3): 298–311.
- Di Stefano G, Pandolfi L, Petronio C *et al.* 2015. The morphology and the occurrence of *Cervus elaphus* (mammalia, cervidae) from the Late Pleistocene of the Italian peninsula. *Rivista Italiana di Paleontologia e Stratigrafia* **121**(1). <https://doi.org/10.13130/2039-4942/6402>
- Driesch Avonden. 1976. *A Guide to the Measurement of Animal Bones from Archaeological Sites*. Harvard University Press: Cambridge MA.
- Driesch A, von den, Boessneck J. 1995. Final report on the zooarchaeological investigation of animal bone finds from Tell Hesban, Jordan. In *Hesban, Faunal Remains: Taphonomic and Zooarchaeological Studies of the Animal Remains from Tel Hesban and Vicinity*, LaBianca OS, von den Driesch A (eds). Andrews University Press: Berriens Spring.
- Eisenmann V. 1986. Comparative osteology of modern and fossil horses, half-asses, and asses. In *Equids in the Ancient World 1*, Meadow RH, Uerpmann HP (eds). Reichert: Wiesbaden; 67–116.
- Eisenmann V. 1992. Systematic and biostratigraphical interpretation of the equids from Qafzeh, Tabun, Shkul and Kebara (Archeuloyabrudian to Upper Paleolithic of Israel). *Archaeozoologia* **5**(1): 43–62.
- Eisenmann V. 2000. *Equus capensis* (Mammalia, Perissodactyla) from Elandsfontein. *Palaeontologia Africana* **36**: 91–96.
- Eisenmann V. 2006. Pliocene and Pleistocene equids: palaeontology versus molecular biology. In *Late Neogene and Quaternary Biodiversity and Evolution*, Kahlke R-D, Maul LC, Mazza PP (eds). Courier Forschungsinstitut Senckenberg: Band 25671–89.
- Eisenmann V. 2012b. Geshar Benot Ya'akov, Israël. Unpublished Report, 23 February 2012. <https://vera-eisenmann.com/-gesher-benot-ya-akov-israel-?lang=en>
- Eisenmann V. 2014. Equus From Melka Kunturé. Unpublished Tables, 17 November 2014. <https://vera-eisenmann.com/equus-from-melka-kunture-tables>
- Eisenmann V. 2020. Sidi Abderrhaman (Afrique du Nord, Rabat, Sidi Abderrhaman, Tihodaïne). Unpublished Report, 15 March 2020. <https://vera-eisenmann.com/-afrique-du-nord-rabat-sidi-abderrhaman-tihodaine-filfila->
- Eisenmann V, Baylac M. 2000. Extant and fossil *Equus* (Mammalia, Perissodactyla) skulls: A morphometric definition of the subgenus *Equus*. *Zoologica Scripta* **29**: 89–100.
- Enzel Y, Bar-Yosef O. (eds). 2017. *Quaternary of the Levant*. Cambridge University Press: Cambridge.
- Erbaeva MA. 1988. *Piščuchi kajnozoja (taksonomija, sistematika, filogenija)* [Cenozoic Pikas (Taxonomy, Systematics, Phylogeny)]. Nauka, Moskva. (in Russian).
- Faith TJ, Lyman RL. 2019. *Paleozoology and Paleoenvironments: Fundamentals, Assumptions, Techniques*. Cambridge University Press: Cambridge.
- Fernández JY, Andrews P. 2016. *Atlas of Taphonomic Identifications*. Springer: Dordrecht.
- Fisher JW, Parkington J. 2020. Season of occupation of Elands Bay Cave: Expanding the rock hyrax calendar. *South African Archaeological Bulletin* **212**: 27–36.
- Fortelius M, Mazza PA, Sala BE. 1993. *Stephanorhinus* (Mammalia: Rhinocerotidae) of the western European Pleistocene, with a revision of *S. etruscus* (Falconer, 1868). *Palaeontographia Italica* **80**(6): 63–155.
- Garrod DAE, Bate D. 1937. *The Stone Age of Mount Carmel. Excavations at the Wadi el Mughara (1)*. Clarendon: Oxford.
- Gentry AW. 2010. Bovidae. In *Cenozoic Mammals of Africa*, Werdelin L, Sanders WJ (eds). University of California Press: Berkeley; 747–803.
- Gilead D. 1970. *Early Palaeolithic Cultures in Israel and the Near East*. Unpublished PhD thesis, Hebrew University, Jerusalem.
- Goren-Inbar N, Feibel CS, Verosub KL *et al.* 2000. Pleistocene milestones on the out-of-Africa corridor at Geshar Benot Ya'akov, Israel. *Science* **289**(5481): 944–947.
- Goren-Inbar N, Speth JD. 2004. *Human Paleoecology in the Levantine Corridor*. Oxbow Books: Oxford.
- Guérin C. 1980. Les rhinoceros (Mammalia, Perissodactyla) du Miocene terminal au Pleistocene superieur en Europe occidentale: Comparaison avec les especes actuelles. *Documents du Laboratoire de Géologie de la Faculté des Sciences de Lyon* **79**: 1–1182.
- Guérin C. 1986. Le Rhinocéros (Mammalia, Perissodactyla) du Pléistocène ancien d'Oubeidiyeh (Israël). *Mémoires et Travaux du Centre Recherche Français en Jérusalem* **5**: 593–598.
- Haas G. 1951. Remarques sur la microfaune de mammifères de la grotte d'Oumm Qatafa. In *La Paleolithique et Le Mesolithique Du Desert de Judée*, Neuville R (ed.). Masson, 218–233.
- Halstead P, Collins P, Isaakidou V. 2002. Sorting the sheep from the goats: morphological distinctions between the mandibles and mandibular teeth of adult *Ovis* and *Capra*. *Journal of Archaeological Science* **29**(5): 545–553.
- Hammer Ø, Harper DAT, Ryan PD. 2001. PAST: Paleontological statistics software package for education and data analysis. *Palaeontologia Electronica* **4**: 9.

- Heptner VG, Nasimovich AA, Bannikov AG. 1988. *Mammals of the Soviet Union. Artiodactyla and Perissodactyla*. Smithsonian Institution Libraries and the National Science Foundation: Washington DC.
- Hershkovitz I, Weber GW, Quam R *et al.* 2018. The earliest modern humans outside Africa. *Science* **359**(6374): 456–459.
- Hershkovitz I, Marder O, Ayalon A *et al.* 2015. Levantine cranium from Manot Cave (Israel) foreshadows the first European modern humans. *Nature* **520**(7546): 216–219.
- Hijmans RJ. 2021. terra: Spatial Data Analysis. R package version 1.5-8. <https://rspatial.org/terra/>
- Hooijer DA. 1961. The fossil vertebrates of Ksar' Akil, a palaeolithic rock shelter in the Lebanon. *Zoologische Verhandlungen* **49**: 3–68.
- Horowitz A. 1988. Quaternary environments and paleogeography in Israel. In *The Zoogeography of Israel*, Yom-Tov Y, Tchernov E (eds). Dr. W. Junk Publishers: Dordrecht; 35–58.
- Horowitz A. 1989. Continuous pollen diagrams for the last 3.5 m.y. from Israel: vegetation, climate and correlation with the oxygen isotope record. *Palaeogeography, Palaeoclimatology, Palaeoecology* **72**: 63–78.
- Horowitz A. 1992. *Palynology of Arid Lands*. Elsevier Science.
- Horowitz LK, Cope C, Tchernov E. 1980. Sexing the bones of mountain-gazelle (*Gazella gazella*) from prehistoric sites in the southern Levant. *Paléorient* **16**(2): 1–12.
- Horowitz LK, Smith P. 1988. The effects of striped hyaena activity on human remains. *Journal of Archaeological Science* **15**: 471–482.
- Horowitz LK, Goldberg P. 1989. A study of Pleistocene and Holocene hyaena coprolites. *Journal of Archaeological Science* **16**: 71–94.
- Horowitz LK, Chazan M. 2007. Holon in the context of the Levantine Lower Paleolithic. In *The Lower Paleolithic Site of Holon, Israel*, Chazan M, Horowitz LK (eds). American School of Prehistoric Research Bulletin 50. Peabody Museum of Archaeology and Ethnology: Cambridge; 181–191.
- Horowitz LK, Monchot H. 2007. Sus Hippopotamus, Bos and Gazella. In *Holon: A Lower Paleolithic Site in Israel*, Chazan M, Horowitz LK (eds). Peabody Museum, Harvard University: MA; 91–105.
- Horowitz LK, Smith P, Faerman M *et al.* 2011. The Application of biometry and LA-ICP-MS to provenance isolated bones: a study of hominin remains from Oumm Qatafa Cave, *Archaeological and Anthropological Sciences* **3**(3): 245–262.
- Jelinek AJ, Farrand WR, Haas G *et al.* 1973. New excavations at the Tabun Cave, Mount Carmel, Israel, 1967–1972: a preliminary report. *Paléorient* **1**(2): 151–183.
- Khaki Sahneh S, Nouri Z, Alizadeh Shabani A *et al.* 2014. A review on habitats selection by Afghan Pika (*Ochotona rufescens*), case study: the Lashgardar protected area in Hamadan Province. *Journal on New Biological Reports* **3**(3): 186–199.
- Klein RG, Cruz-Uribe K. 1984. *The Analysis of Animal Bones from Archeological Sites*. University of Chicago Press: Chicago.
- Klein RG, Cruz-Uribe K. 1996. Size variation in the rock hyrax (*Procapra capensis*) and Late Quaternary climatic change in South Africa. *Quaternary Research* **46**(2): 193–207.
- Kuhn BF, Berger IR, Skinner JD. 2010. Examining criteria for identifying and differentiating fossil faunal assemblages accumulated by hyenas and hominins using extant hyenid accumulations. *International Journal of Osteoarchaeology* **20**: 15–35.
- Kurtén B. 1965. The carnivora of the palestine caves. *Acta Zoologica Fennica* **107**: 3–74.
- Lacombat F. 2006. Morphological and biometrical differentiation of the teeth from Pleistocene species of *Stephanorhinus* (Mammalia, Perissodactyla, Rhinocerotidae) in Mediterranean Europe and the Massif Central, France. *Palaeontographica* **274**: 71–111.
- Lazagabaster IA, Ullman M, Porat R *et al.* 2021a. Changes in the large carnivore community structure of the Judean Desert in connection to Holocene human settlement dynamics. *Scientific reports* **11**(1): 1–11.
- Lazagabaster IA, Rovelli V, Fabre PH *et al.* 2021b. Rare crested rat subfossils unveil Afro–Eurasian ecological corridors synchronous with early human dispersals. *Proceedings of the National Academy of Sciences* **118**(31): e2105719118.
- Lazagabaster IA, Égüez N, Ullman M *et al.* 2022. Cave paleozoology in the Judean Desert: assembling records of Holocene wild mammal communities. *Journal of Quaternary Science*. <https://doi.org/10.1002/jqs.3405>
- Lebon M, Reiche I, Fröhlich F *et al.* 2009. Characterization of archaeological burnt bones: contribution of a new analytical protocol based on derivative FTIR spectroscopy and curve fitting of the $\nu 1 \nu 3$ PO4 domain. *Analytical and Bioanalytical Chemistry* **392**: 1479–1488.
- Lister AM. 1996. The morphological distinction between bones and teeth of fallow deer (*Dama dama*) and red deer (*Cervus elaphus*). *International Journal of Osteoarchaeology* **6**: 119–143.
- Lyman RL. 1986. On the analysis and interpretation of species list data in zooarchaeology. *Journal of Ethnobiology* **6**(1): 67–81.
- Lyman RL. 1995. *Vertebrate Taphonomy*. Cambridge University Press: Cambridge.
- Lyman RL. 2015. The history of “laundry lists” in North American zooarchaeology. *Journal of Anthropological Archaeology* **39**: 42–50.
- Lyman RL. 2016. Holocene mammalian change in the central Columbia Basin of eastern Washington State, USA. *Quaternary Science Reviews* **146**: 66–76.
- Marder O, Yeshurun R, Lupu R *et al.* 2011. Mammal remains at Rantis Cave, Israel, and Middle–Late Pleistocene human subsistence and ecology in the Southern Levant. *Journal of Quaternary Science* **26**(8): 769–780.
- Marean CW, Anderson RJ, Bar-Matthews M *et al.* 2015. A new research strategy for integrating studies of paleoclimate, paleoenvironment, and paleoanthropology. *Evolutionary Anthropology* **24**(2): 62–72.
- Martínez-Navarro B, Belmaker M, Bar-Yosef O. 2009. The large carnivores from 'Ubeidiya (early Pleistocene, Israel): biochronological and biogeographical implications. *Journal of Human Evolution* **56**(5): 514–524.
- Martínez-Navarro B, Rabinovich R. 2010. The fossil Bovidae (Artiodactyla, Mammalia) from Gesher Benot Ya'aqov, Israel: out of Africa during the Early–Middle Pleistocene transition. *Journal of Human Evolution* **60**(4): 375–386.
- Martínez-Navarro B, Belmaker M, Bar-Yosef O. 2012. The Bovid assemblage (Bovidae, Mammalia) from the Early Pleistocene site of 'Ubeidiya, Israel: Biochronological and paleoecological implications for the fossil and lithic bearing strata. *Quaternary International* **267**: 78–97.
- Maul LC, Smith KT, Shenbrot G *et al.* 2015. Microvertebrates from unit G/layer 17 of the archaeological site of Hummal (El Kowm, Central Syria): Preliminary results. *L'Anthropologie* **119**(5): 676–686.
- Maul LC, Bruch AA, Smith KT *et al.* 2016. Palaeoecological and biostratigraphical implications of the microvertebrates of Qesem Cave in Israel. *Quaternary International* **398**: 219–232.
- Meignen L, Bar-Yosef O, Goldberg P *et al.* 2000. Le feu au Paléolithique moyen: recherches sur les structures de combustion et le statut des foyers. L'exemple du Proche-Orient. *Paléorient* **26**(2): 9–22.
- Mendelssohn H, Yom-Tov Y. 1999. *Fauna Palaestina: Mammalia of Israel*. Jerusalem, The Israel Academy of Sciences and Humanities.
- Montes L, Blasco F. 1997. Los hiénidos del yacimiento musteriano de Gabasa 1 (Huesca, España). *Bolskan* **14**: 9–27.
- Neuville R. 1931. L'Acheuléen supérieure de la grotte d'Oumm Qatafa (Palestine). *L'Anthropologie* **41**(13–51): 249–263.
- Neuville R. 1934. Le préhistorique de Palestine. *Revue Biblique* **43**(2): 237–259.
- Neuville R. (ed.). 1951. *Paléolithique et Mésolithique du Désert de Judée*. Archives de l'Institut de Paléontologie Humaine 24. Masson: Paris.
- Neuville R, Mallon A. 1931. Les debuts de l'âge des métaux dans les grottes du désert de Judée. *Syria* **12**: 24–47.
- Neuville R, Boureau R. 1930. Squelettes palestiniens du premier âge du Bronze. *Bulletins et Mémoires de la Société d'Anthropologie de Paris* **1**(4–6): 33–36.
- Nowell A, Walker C, Cordova CE, Ames CJH, Pokines J, Stueber D, DeWitt R, Al-Souliman ASA. 2016. Middle Pleistocene subsistence in the Azraq Oasis, Jordan: Protein residue and other proxies. *Journal of Archaeological Science* **73**: 36–44.
- Orbach M, Yeshurun R. 2019. The hunters or the hunters: Human and hyena prey choice divergence in the Late Pleistocene Levant. *Journal of Human Evolution* **160**: 102572.

- Pandolfi L. 2018. Evolutionary history of Rhinocerotina (Mammalia, Perissodactyla). *Fossilia* **2018**: 27–32.
- Pandolfi L, Tagliacozzo A. 2015. Stephanorhinus hemitoechus (Mammalia, Rhinocerotidae) from the Late Pleistocene of Valle Radice (Sora, Central Italy) and re-evaluation of the morphometric variability of the species in Europe. *Geobios. Memoire Special* **48**(2): 169–191.
- Pandolfi L, Cerdeño E, Codrea V *et al.* 2017. Biogeography and chronology of the Eurasian extinct rhinoceros *Stephanorhinus etruscus* (Mammalia, Rhinocerotidae). *Comptes Rendus. Palevol* **16**(7): 762–773.
- Pandolfi L, Rivals F, Rabinovich R. 2020. A new species of rhinoceros from the site of Bethlehem: “Dihoplus” bethlehemsis sp. nov. (Mammalia, Rhinocerotidae). *Quaternary International* **537**: 48–60.
- Payne S. 1973. Kill-off patterns in sheep and goats: the mandibles from Aşvan Kale. *Anatolian Studies* **23**: 281–303.
- Payne S. 1988. Animal bones from Tell Rubeidheh. In *Tell Rubeidheh: An Uruk Village in the Lebel Hamrin*, Killick RG (ed.). Iraq Archaeological Reports 2. Aris & Phillips: Warminster; 98–135.
- Perrot J. 1992. Umm Qatafa and Umm Qala'a: two Ghassulian caves in the Judean desert. *Eretz-Israel* **23**: 100–111.
- Phillips S. 2021. maxnet: Fitting 'Maxent' Species Distribution Models with 'glmnet'. R package version 0.1.4. <https://CRAN.R-project.org/package=maxnet>
- Porat N, Chazan M, Schwarcz HP *et al.* 2002. Timing of the Lower to Middle Paleolithic transition in the Levant: evidence from new dates. *Journal of Human Evolution* **43**: 107–122.
- Porat N, Schwarcz H, Tchernov E *et al.* 1992. The chronostratigraphy of the tool-bearing layers at Oumm Qatafa cave (Judea Desert), revisited. Abstract, Annual Meeting, the Israel Geological Society; 116–117.
- Potts R, Behrensmeyer AK, Tyler FJ *et al.* 2018. Environmental dynamics during the onset of the Middle Stone Age in eastern Africa. *Science* **360**(6384): eaao2200.
- Prummel W. 1988. Distinguish features on postcranial skeletal elements of cattle, *Bos primigenius Taurus Cervus elaphus* f., and red deer. Schriften Aus Der Archäologisch- Zoologischen Arbeitsgruppe Schleswig-Kiel 12 (AZA), 52.
- Rabinovich R, Biton R. 2011. The early–middle pleistocene faunal assemblages of Gesher Benot Ya 'aqov: Inter-site variability. *Journal of human evolution* **60**(4): 357–374.
- Rabinovich R, Gaudzinski-Windheuser S, Goren-Inbar N. 2008. Systematic butchering of fallow deer (*Dama*) at the early Middle Pleistocene Acheulian site of Gesher Benot Ya'aqov (Israel). *Journal of Human Evolution* **54**: 134–149.
- Rabinovich R, Ackermann O, Aladjem E *et al.* 2012. Elephants at the Middle Pleistocene Acheulian open-air site of Revadim Quarry, Israel. *Quaternary International* **276–277**: 183–197.
- Rey C, Miquel JL, Facchini L *et al.* 1995. Hydroxyl groups in bone mineral. *Bone* **16**: 583–586.
- Rohlf JF. 2017. TPSdig (Version 2.31) [Windows]. <https://sbmorphometrics.org/morphmet/tpsdig2w64.exe>
- Rolland N. 2004. Was the emergence of home bases and domestic fire a punctuated event? A review of the Middle Pleistocene record in Eurasia. *Asian Perspectives* **43**(2): 248–280.
- Sam Y. 2020. African origins of modern asses as seen from paleontology and DNA: what about the Atlas wild ass? *Geobios* **58**: 73–84.
- Sauqué V, Gisbert M, de Torres T *et al.* 2017. Pleistocene cave hyenas in the Iberian Peninsula: New insights from Los Apendices Cave (Moncayo, Zaragoza). *Palaeontologia Electronica* **20**(1): 11A.
- Scardia G, Parenti F, Miggins DP *et al.* 2019. Chronologic constraints on hominin dispersal outside Africa since 2.48 Ma from the Zarqa Valley, Jordan. *Quaternary Science Reviews* **219**: 1–19.
- Sen S, Delfino M, Kazanci N. 2017. Çeştepe, a new early Pliocene vertebrate locality in Central Anatolia and its stratigraphic context. *Annales de Paléontologie* **103**(2): 149–163.
- Shahack-Gross R, Bar-Yosef O, Weiner S. 1997. Black-coloured bones in Hayonim Cave, Israel: Differentiating between burning and oxide staining. *Journal of Archaeological Science* **24**(5): 439–446.
- Shahack-Gross R, Berna F, Karkanas P *et al.* 2014. Evidence for the repeated use of a central hearth at Middle Pleistocene (300 ky ago) Qesem Cave, Israel. *Journal of Archaeological Science* **44**: 12–21.
- Shemer M, Crouvi O, Shaar R *et al.* 2019. Geochronology, paleogeography and archaeology of the Acheulian locality of 'Evron Landfill in the Western Galilee, Israel. *Quaternary Research* **91**(2): 729–750.
- Shimelmitz R, Kuhn SL, Jelinek AJ *et al.* 2014. “Fire at will”: The emergence of habitual fire use 350,000 years ago. *Journal of Human Evolution* **77**: 196–203.
- Silver IA. 1969. The ageing of domestic animals. Science in Archaeology, Brothwell D, Higgs E (eds). Thames & Hudson: London; 283–302.
- Smith AT. 2020. Conservation status of American pikas (*Ochotona princeps*). *Journal of Mammalogy* **101**(6): 1466–1488.
- Stampfli HR. 1963. Wisent, *Bison bonasus Bos primigenius Bos taurus Seeberg Burgäschisse-Süd* (Linné, 1758), Ur, Bojanus, 1827, und Hausrind, Linné, 1758. In: Boessneck J, Jéquier J-P, Stampfli HR (eds). Teil 3; 117–196.
- Stiner MC, Kuhn SL, Weiner S *et al.* 1995. Differential burning, recrystallization, and fragmentation of archaeological bone. *Journal of Archaeological Science* **22**(2): 223–237.
- Stiner MC, Howell FC, Martinez-Navarro B *et al.* 2001. Outside Africa: Middle Pleistocene *Lycaon* from Hayonim Cave, Israel. *Bollettino Societa Paleontologica Italiana* **40**(2): 293–302.
- Stiner MC, Barkai R, Gopher A. 2009. Cooperative hunting and meat sharing 400–200 kya at Qesem Cave, Israel. *Proceedings of the National Academy of Science of the United States of America* **106**(32): 13207–13212.
- Suchentrunk F, Alkon PU, Willing R *et al.* 2000. Epigenetic dental variability of Israeli hares (*Lepus* sp.): ecogenetic or phylogenetic causation? *Journal of Zoology* **252**: 503–515.
- Taylor LA, Kaiser TM, Schwitzer C *et al.* 2013. Detecting inter-cusp and inter-tooth wear patterns in Rhinocerotids. *PLoSOne* **8**(12): e80921.
- Tchernov E. 1962. Paleolithic avifauna in Palestine. *Bulletin of the Research Council of Israel* **11**: 95–131.
- Tchernov E. 1968. *Succession of Rodent Faunas during the Upper Pleistocene of Israel*. Paul Parey: Hamburg & Berlin.
- Tchernov E. 1988. The biogeographical history of the Southern Levant. In *The Zoogeography of Israel*, Yom-Tov Y, Tchernov E (eds). Dr. W. Junk Publishers, Kluwer Academic Publishers: Dordrecht; 159–250.
- Tchernov E. 1992. The Afro-Arabian component in the Levantine mammalian fauna—a short biogeographical review. *Israel Journal of Zoology* **38**(3–4): 155–192.
- Tchernov E. 1998. The faunal sequences of the Southwest Asian Middle Paleolithic in relation to hominid dispersal events. In *Neandertals and Modern Humans in Western Asia*, Akazawa T, Aoki A, Bar-Yosef O (eds). Plenum: New York; 77–90.
- Tchernov E, Tsoukala E. 1997. Middle Pleistocene (Early Toringian) Carnivore Remains from Northern Israel. *Quaternary Research* **48**: 122–136.
- Uerpmann H-P. 1987. *The ancient distribution of ungulate mammals in the Middle East*. Dr. Ludwig Reichert Verlag: Wiesbaden.
- Vaufrey E. 1931. Paleontologie. In *L'Acheuléen supérieure de la grotte d'Oumm Qatafa (Palestine)* L'Anthropologie, Neuville R (ed.). **41**(13–51): 253–263.
- Vaufrey R. 1951. Etude Paleontologique. In *Le Paleolithique et Le Mesolithique Du Dsesert de Judée*, Neuville R (ed.). Archives de l'Institute de Paleontologie Humaine, Memoire 24. Masson: Paris; 198–217.
- Villa P, Mahieu E. 1991. Breakage patterns of human long bones. *Journal of Human Evolution* **21**(1): 27–48.
- Werdelin L, Lewis ME. 2008. New species of *Crocota* from the early Pliocene of Kenya, with an overview of early Pliocene hyenas of eastern Africa. *Journal of Vertebrate Paleontology* **28**(4): 1162–1170.
- Werdelin L, Solounias N. 1991. The Hyaenidae: taxonomy, systematics and evolution. *Fossils and Strata* **30**: 1–104.
- Willis KJ, Bailey RM, Bhagwat SA *et al.* 2010. Biodiversity baselines, thresholds and resilience: testing predictions and assumptions using palaeoecological data. *Trends in Ecology & Evolution* **25**(10): 583–591.
- Wojtczak DB, Le, Tensorer J-M. 2018. The long Paleolithic sequence of Hummal (Central Syria). In *Proceedings of Iscach, Beirut 2015*. Open Access: <http://Www.Archaeopress.Com/Archaeopressshop/>

- Public/Displayproductdetail.Asp?Id={1269D8F3-5DD6-4B1B-BC5A-1746E604CB17}
- Wurz S, van Peer P. 2012. Out of Africa, The Nile Valley and the Northern Route. *South African Archaeological Bulletin* **67**(196): 168–179.
- Yom-Tov Y. 1967. On the taxonomic status of the hares (Genus *Lepus*) in Israel. *Mammalia* **31**(2): 246–259.
- Yom-Tov Y, Mendelssohn. 1999. *The Mammalia of Israel*. Israel Academy of Sciences and Humanities: Jerusalem.
- Yeshurun R, Zaidner Y, Eisenmann V *et al.* 2011. Lower Paleolithic hominin ecology at the fringe of the desert: Faunal remains from Bizat Ruhama and Nahal Hesi, Northern Negev, Israel. *Journal of Human Evolution* **60**: 492–507.
- Zack SP. 2012. Deciduous dentition of Didymictis (Carnivoramorpha: Viverravidae): implications for the first appearance of “Creodonta. *Journal of Mammalogy* **93**(3): 808–817.
- Zeder MA, Lapham HA. 2010. Assessing the reliability of criteria used to identify postcranial bones in sheep, *Ovis*, and goats, *Capra*. *Journal of Archaeological Science* **37**(11): 2887–2905.
- Zohary M. 1973. *Geobotanical Foundations of the Middle East*. Gustav Gischer Verlag: Stuttgart; Swet and Zeitlinger: Amsterdam.